Master thesis

EVALUATION OF A NOVEL SENSOR SYSTEM INTEGRATED INTO A MOSQUITO TRAP TO DETERMINE MOSQUITO SPECIES, AGE AND SEX

September 2018

MASTER IN ZOONOSES AND ONE HEALTH

2017-2018

Author**: Josep Brosa Casanovas**

Directors:

Carles Aranda

Sandra Talavera

Núria Busquets

Collaborators:

Evaluation of a novel sensor system integrated into a mosquito trap to determine mosquito species, age and sex

Master thesis

September 2018

MASTER IN ZOONOSES AND ONE HEALTH

2017-2018

Author: Josep Brosa Casanovas

Directors: Carles Aranda, Sandra Talavera, Núria Busquets

Collaborators: Irideon S.L.

Author signature	Director signature	Director signature	Director signature
Josep Brosa	Carles Aranda	Sandra Talavera	Núria Busquets

ACKNOWLEDGEMENTS

I wish to express my sincere gratitude to my directors Carles Aranda, Sandra Talavera and Núria Busquets for their support and help that made this project possible and to all the entomology team of CReSA for their kindness and help whenever I needed it.

I would like to thank the Irideon collaborators Joao Encarnacao, Bastian Faulhaber and Mark Williams for their implication in the project.

I also want to thank Sebastian Napp for his significant help with the statistical part of the project.

And last, but not least, I want to thank Anna Vila for the support in the design and her patience.

ACRONYMS

BSL	Biosafety level
MFCC	Mel Frequency Cepstral Coefficient
PSD	Power Spectral Density
rms	Root mean square
VBD	Vector-borne diseases

CONTENTS

ABSTRACT

Important vector borne zoonotic diseases are transmitted by different mosquito species. Mosquito surveillance needs expert entomologists and is time-consuming. Trap-captured mosquitoes are transported to the laboratory for counting and identification, and there are over 3,500 species of mosquitoes in the world. In order to improve mosquito surveillance, we evaluated the accuracy of a novel optoelectronic sensor prototype that captures the shadow of the mosquito while is being sucked into a trap. This is the first time that species, sex and age classification of mosquitoes is made with the forced flight condition of a commercial ventilator-based mosquito trap, where the natural wing-beat is distorted. *Culex pipiens*, *Aedes albopictus* and *Aedes aegypti* were used to test the sensor. Various algorithms on different feature combinations were trained and optimized for machine learning to recognize automatically mosquitoes' sex, age and species. Our system was capable to distinguish between species and sex in terms of fundamental frequency, showing that the fundament frequency was higher in males than females and higher in mosquitoes of *Aedes* than in *Culex* genus. The system proposed in this study is useful for genus classification with accuracy values that ranged from 93.83% to 95.73%. More data and training will be necessary to optimize the sensor to better classify mosquito species of the same genus since the accuracy for *Aedes* genus was 76.06%. Regarding gender identification, male and female were discriminated with more than 93.11% of accuracy after machine learning techniques. This information will be important for arbovirus surveillance programs since the females are the unique implied in arbovirus transmission. The accuracy in terms of age ranged from 69.81% to 90.97%, allowing to know how old the mosquito population is, providing useful data due to the importance of the age in vector capacity which it is important to estimate the risk assessment for arbovirus diseases.

Introduction

Every year more than one billion people are infected, and more than one million people die because of vector-borne diseases (VBD) (malaria, dengue, yellow fever, schistosomiasis, leishmaniasis, Chagas disease, lymphatic filariasis, onchocerciasis, and many other different VBD) (WHO, 2014). Approximately 30% of the world's human population still lives with the threat of insect-borne disease (Becker *et al.*, 2010). A world increasingly connected through travel, trade and tourism is an important factor for VBD spreading such as dengue, West Nile fever, yellow fever, chikungunya and malaria, all of them transmitted by mosquitoes (Lee *et al.* 2013, ECDC, 2014). Climate change and global warming may contribute to more favorable conditions for survival and life cycle completion of the vector (Rossati, 2017), but climate warming does not necessarily lead to an increase in mosquito abundance (Roiz *et al*., 2014) and furthermore, temperature alters the replication of the virus in the mosquito and infection rates (Kilpatrick *et al.*, 2008). Moreover, the effects of climate are species-specific, place-specific and non-linear (Roiz *et al.*, 2014). This specificity requires tailored parameters for individual vector-pathogen systems to more accurately project the impact of climatic changes on VBD transmission (Parham *et al.* 2015).

Important vector borne zoonotic diseases are transmitted by different mosquito species. There are over 3,500 species of mosquitoes in the world (Mosquito Catalog, 2018), mainly belonging to the *Culex, Aedes* and *Anopheles* genera. *Aedes aegypti* and *Aedes albopictus* species can transmit Chikungunya, dengue, yellow fever and Zika viruses. In the case of *Ae. albopictus*, it can also transmit Rift Valley fever and West Nile viruses (Brustolin *et al*., 2016 and Brustolin *et al*., 2017). Both mosquito species are two of the most invasive mosquito species and are important vectors of arboviruses. *Aedes aegypti* is predicted to occur primarily in the tropics and sub-tropics, but with relatively few areas of possible suitability in some Mediterranean countries and temperate North America. *Aedes albopictus* distribution extends into southern Europe, northern China, southern Brazil, northern United States, and Japan (Kraemer *et al.*, 2015). This reflects *Ae. albopictus* ability to tolerate lower temperatures (Brady *et al., 2013)*. In general, *Ae. aegypti* develops preferably in urban areas due its antropophily, endophily and endophagy, while *Ae. albopictus* can be found spread anywhere limited only to the presence of their particular breeding sites, common in cemeteries and containers in humanized zones (Valdés *et al.*, 2009 and Caputo *et al.*, 2012). In certain areas, habitat segregation in terms of distance from the coast can influence its distribution. Frequently they fight over their distribution zones, which often causes the competitive displacement of one of the species (Rey

and Lounibos 2015). In Europe and other temperate and tropical regions, members of the *Culex pipiens* complex are the most ubiquitous mosquito species which serve as principal vectors for various arboviruses such as Rift Valley fever and West Nile viruses (Rudolf *et al*., 2013, WHO 2014). *Culex pipiens* global distribution combined with their mixed feeding patterns on birds and mammals (including humans), increases the transmission of several avian viruses to humans (Farajollahi, 2011). *Culex pipiens* species is formed by two biotypes, pipiens and molestus, which can form hybrids. Both biotypes and their hybrids are morphologically identical but differ in their behavior (Vogels 2017). The typical pipiens biotype prefers birds as host, diapauses during winter, mates in swarms and requires a blood meal prior to egg laying (anautogenous) (Byrne & Nichols 1999). The molestus biotype prefers mammals as host, can remains active year-round, mates in confined spaces and can lay its first egg batch without a blood meal (autogenous) (Rudolf *et al.*, 2013). Hybrid forms fed on birds and mammals, and human bloodmeals are common, predisposing them to serve as potential bridge vectors from birds to humans (Medlock *et al*., 2005). The considerable presence of hybrids in peri- urban areas suggests that these urban borders may represent high- level hybridization zones, in which conditions support the co- occurrence and interbreeding of molestus and pipiens forms. Molestus form typically occupies underground and confined breeding habitats in peri-urban areas (Osório, 2014). To sum up, invasive and native mosquitoes are vectors of pathogens with high human and veterinary relevance and entomological surveillance belongs to animal and human disease surveillance within the 'One Health' concept where interdisciplinary collaboration and communication in healthcare for humans and animals is crucial (ECDC 2014 and ECDC 2012).

Adult mosquitoes share the characteristic of most Diptera in having a single pair of wings and they are relatively strong fliers. Wing characters provide useful information for identifying the sex of culícids (Virginio *et al*., 2015). Mosquito adults are small flying midge-like insects with long, slender wings (Eldridge, 2005). Mosquito flight is powered by indirect flight muscles, which produce wing strokes by deforming the thoracic box. These are asynchronous fibrillar muscles. Most female mosquitoes have long, slender proboscis that is adapted for piercing skin and sucking blood. Male mosquitoes also have a proboscis, but it is adapted for sucking plant juices and other sources of sugars. Most male mosquitoes are generally smaller than females of the same species and have much longer maxillary palps and bigger and hairier antenna. The bodies of mosquito adults are covered with small scales, often with patterns of contrasting colors. These patterns are used to identify morphologically mosquitoes to species. The wing-

beat frequencies of males are always higher than females (Clements, 1992), but mosquitoes sometimes modulate their flight tone to communicate. For some species, male and female flight harmonics converge toward a common frequency while mating (Genoud *et al*., 2018). Tones are detected by the antennae of the male, which are more sensitive to vibration (Arthur *et al.*, 2014). The characteristics of mosquito wingbeat were studied through acoustic, optical, and radar approaches, but there are certain difficulties for implementing a robust system for in-field mosquito population monitoring using these methods and due to the tinny size of the study subject, the optical methods suffered from the resolution of the sensor. With the rapid progress of computers, automatic classification algorithms were introduced in the studies on insect wingbeat (Ouyang, 2015).

Mosquito surveillance consists in routine monitoring of both larval and adult mosquito populations over the course of an entire mosquito season. It is critical to a successful mosquito control program. Mosquito surveillance program allow: i) monitoring changes in mosquito populations, ii) identifying which mosquito species are present, allowing the identification of new invasive species, iii) detecting mosquito-borne diseases and iv) determining what control measures need to be conducted (Flores, 2005). This kind of surveillance needs expert entomologists and is time-consuming because of specialist technicians set adult mosquito traps and the mosquitoes captured are transported to the laboratory for counting and identification.

The purpose of the present study is to evaluate the accuracy of a novel optoelectronic sensor prototype that can capture the shadow of the mosquito is being sucked into the trap by the ventilator of a commercial trap. In the literature, basic wing-beat studies have been reported for mosquitoes in free flight (Villarreal *et al.*, 2017, Arthur *et al.*, 2013, Cator *et al.*, 2012 and Iams, 2012), but this is the first time that species, age and sex classification of mosquitoes is made with the forced flight condition of a commercial ventilator-based mosquito trap, where the natural wing-beat is distorted making it insufficient for species classification until now. *Culex pipiens*, *Ae. albopictus* and *Ae. aegypti* species were used to asses it. With this data, machine learning techniques were used to develop pipelining techniques that enables the sensor to always recognize automatically the sex, age and species.

Material and methods

Mosquito rearing

The colonies used for the sensor testing were: i) *Cx. pipiens* 2012 strain Gavà, Barcelona, Spain (41.3º, 2.0167º), ii) *Ae. albopictus*, 2005 strain Sant Cugat del Vallès, Barcelona, Spain

(41.4667º, 2.0833º) and iii) *Ae. aegypti* 1994 strain Paea, Tahiti, French Polynesia (-17.688889°, -149.586944°). *Culex pipiens* and *Ae. albopictus* were reared in biosafety level 2 (BSL2) laboratory and *Ae. aegypti* in biosafety level 3 (BSL3) laboratory at CReSA-IRTA facilities.

Culex pipiens, *Ae. albopictus* and *Ae. aegypti* immature stages and adults were reared under controlled environmental conditions at 28ºC and 80% RH in climatic chambers, with a photoperiod of 12:12 hours light:dark cycle: 8am to 8pm of light and 8pm to 8am of darkness for *Ae. albopictus* and *Ae. aegypti* and 11am to 11pm of darkness and 11pm to 11am of light for *Cx. pipiens*, with half an hour of twilight in each period.

Larvae were kept in plastic trays with dechlorinated tap water and fed with fish pellets (*Goldfish Sticks* – TETRA) *ad libitum* and water renovation three times a week. Pupae were immediately placed in insect cages (BugDorm-1 Insect Rearing Cage, W30 x D30 x H30 cm). After metamorphosis, adults were fed with sucrose solution (10%) *ad libitum* changed two times a week. Females of all species were never fed with blood to avoid a body-size increase and flight modifications. Sucrose solution (10%) was removed before mosquito transferring to the insect cage with the trap inside to increase their appetite. *Aedes* mosquitoes and *Cx. pipiens* fasted 24 and 48 hours respectively to improve their affinity for the attractant.

Sensor description and data acquisition process

The commercial trap used to test the sensor was "BG-Mosquitaire" from Biogents, Germany. It contained an electrical fan which creates a flow of air down through the entrance funnel in the lid of the trap, and into a catch bag in the body of the trap. The air was then expelled through a white grill at the top of the trap. The trap was fitted with a sachet containing an artificial human scent called BG-Sweetscent, from Biogents AG, whose odor was released with the expelled air to attract mosquitoes to the trap. In this manner, mosquitoes that were flying close to the mouth of the funnel were overpowered by the air flow from the suction fan and were sucked in through the funnel. The sensor was fitted between the entrance funnel of the trap and the body of the trap (Figure 1). In this manner, mosquitoes which were drawn into the funnel by the suction fan were sensed before being trapped in the catch bag. The size of the insect cage where the trap was allocated was W47.5 x D47.5 x H93.0 cm. (BugDorm-4S4590 Insect Rearing Cage).

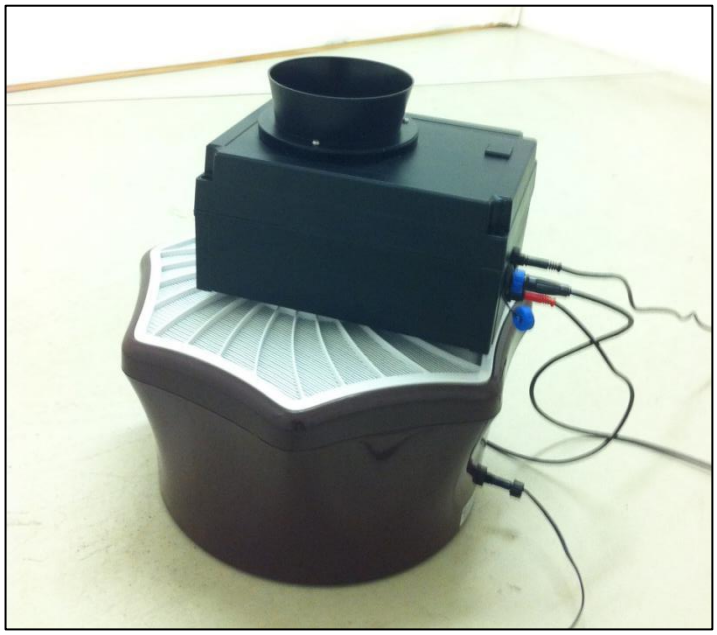

Figure 1, Irideon sensor (rectangular black box) fitted to the top of a BG Mosquitaire mosquito trap (brown cylinder with white lid.

To introduce the mosquitoes into the cage, a mouth aspirator was used in BSL2 conditions and a mechanical aspirator in BSL3 conditions. In this case, *Ae. aegypti* were previously separated by gender in small cages of 10 individuals using carbon dioxide to anesthetize them. The mosquitoes were introduced in batches of 20 in *Cx. pipiens* and *Ae. albopictus* species to avoid saturation of the trap and because the sensor needs a second between each flight. In the case of *Ae. aegypti* the batches were reduced to 10 because they had more affinity to the attractant.

In the Irideon sensor, the optical emitter was formed by a two-dimensional (2D) array of 940 nm wavelength infrared light emitting diodes (LEDs) and optical lenses; and the optical receiver was formed by a two-dimensional (2D) array of 940 nm photodiodes and optical lenses. The sensor had an active length of around 70 mm in the downward direction, corresponding to a sensor *length* of 4 LEDs in the emitter and 4 photodiodes in the receiver. The air flow due to the ventilator in the trap was approximately 3 m/s in the downward direction. The duration of a typical mosquito flight through the field of view of the sensor was around 50 ms, therefore the typical flight speed was 1.4 m/s. The Irideon sensor contained two extinction sensors in a special configuration, so each flight event comprises two 50 ms recordings. A sampling frequency of 9603 samples per second was used on each of the channels. The sensor also recorded the ambient temperature and relative humidity at the time of each fight and tagged each flight with a time stamp, with 1 second resolution.

The sensor box contained electronics and firmware to drive the LEDs, and to amplify and acquire the signal from the photodiodes. When a mosquito entered into the field of view of the sensor, the resultant dip in receiver output triggered a short recording of the sensor output, which also included the receiver output immediately prior to the trigger. At the end of each laboratory experiment, recordings each mosquito flight were downloaded to a laptop via a USB cable. Each recording was in the form of a .csv file that could be imported and viewed in a spreadsheet program such as Microsoft Excel.

To evaluate the wingbeat frequency and accuracy of the prototype optoelectronics sensor, mosquitoes were separated according to species, sex and age. Different ages (2-4 days, 7-9 days and 14-16 days) were tested for each species (*Cx. pipiens*, *Ae. albopictus* and *Ae. aegipty*) and sex (female and male), with a total of 18 conditions were analyzed.

Data analysis

Preprocessing and feature extraction

The preprocessing and feature extraction process prepares the data for the machine learning. It consists of three steps:

i) Audio conversion. The raw data is converted to an audio .wav file for later analysis. A Python script has been developed for this.

ii) Deletion of invalid data. A flight viewer in Python has been developed in order to be able to visualize the audio signal and be able to delete invalid data like false triggers, double flights or cut flights.

iii) Feature extraction. An audio feature extraction library in Python has been developed to extract features from the flight which could be useful for the machine learning. All features, except the MFCC, are extracted from an estimate of the power spectral density (PSD) using Welch's method (Villwock and Pacas, 2008). See Annex I.

Characteristics groups

The features were grouped in groups for reducing the number of characteristics combinations.

- Fresnel: includes Fresnel amplitude, Fresnel frequency and Fresnel power (3 features).
- Harmonic form: includes first harmonic start, first harmonic length, second harmonic start, second harmonic length, third harmonic start and third harmonic length (6 features).

- Harmonic frequencies: includes fundamental frequency, second harmonic frequency and third harmonic frequency (3 features).
- Harmonic powers: includes first harmonic power, second harmonic power, third harmonic power (3 features).
- Mel: includes MFCC and Mel-scaled spectrogram (64 features).
- Peak amplitudes: includes first peak amplitude, second peak amplitude, third peak amplitude (3 features).

Machine learning

Various algorithms on different feature combinations were trained and optimized for machine learning.

i) Logistic Regression
ii) Random Forest
iii) XGBoost
iv) Support Vector Machines
v) Fully connected artificial deep neural network

All the data sets are balanced and 75% of the respective data sets were used for training the model and the other 25% for testing it.

Statistical analysis

Difference between sexes for the different species

First, we evaluated the normality of the frequency parameter in both males and females for the different species using the Shapiro-Wilk test. When data was normally distributed, mean frequencies in males and females mosquitos in a given species were compared using the t-test. When data was non-normally distributed, mean frequencies in males and females mosquitos in a given species were compared using the Wilcoxon rank sum test (=Mann–Whitney U test).

Difference between species within the same sex category

Given the results of the evaluation of normality of the frequency parameter in both males and females for the different species, we applied parametric or non-parametric test to assess the differences in the mean frequencies between species within the same sex category. When data was normally distributed, groups were compared using the ANOVA test, and in case of

significance, post-hoc comparisons were carried out using the Tukey test. When data was normally distributed, groups were compared using the Kruskal-Wallis test, and in case of significance, post-hoc comparisons were carried out using the Dunn's test with Bonferroni correction to adjust for multiple tests (i.e. conservative estimation).

Results and discussion

Efficiency of mosquito rearing

A total of 5,671 *Cx. pipiens*, 4,886 *Ae. albopictus* and 2,053 *Ae. aegypti* larvae were reared to adults for the sensor testing. The percentage of survival of larva to pupa were 89.95% for *Ae. albopictus*, 79.59% for *Ae. aegypti* and 60.41% for *Cx. pipiens* (Table 1). *Cx. pipiens* had less survival during mosquito rearing, different larvae food could be tested to optimize it and to increase the number of pupae after larvae rearing.

Table 1, Mosquito rearing

		Species					
		Culex pipiens		***Aedes albopictus***		***Aedes aegypti***	
		01/03/2018 to 25/06/2018		27/02/25018 to 09/05/2018		04/05/25018 to 18/06/2018	
		Larvae	Pupae	Larvae	Pupae	Larvae	Pupae
Rearing	**1**	1,282	676	492	371	976	830
	2	258	199	2,451	2,159	731	603
	3	600	391	950	918	346	201
	4	2,090	1,204	993	947	-	-
	5	1,441	956	-	-	-	-
Total		5,671	3,426	4,886	4,395	2,053	1,634
% Survival		**60.41**		**89.95**		**79.59**	

Efficency of data acquisition

The adult mosquitoes that were used to test the sensor were 1,155 *Cx. pipiens*, 1,885 *Ae. albopictus*, and 1,178 *Ae. aegypti* (Table 2). In the case of male mosquitoes of 14-16 days of age, there were a smaller number of tested specimens because they do not tend to survive until that age. The percentage of valid recorded of mosquitoes in respect of the total mosquitoes captured in the trap was 86.15% for *Cx. pipiens*, 76.39% for *Ae. albopictus* and 79.97 for *Ae. aegypti*.

Table 2, Number of adult mosquitoes used to test the sensor

	2-4 days old		7-9 days old		14-16 days old		Total mosquitoes captured in the trap	Valid recorded mosquitos (females and males)	Valid recorded vs captured mosquitoes (%)
Species	Male	Female	Male	Female	Male	Female			
Culex pipiens	260	170	280	218	56	171	1,155	995 (494 females and 501 males)	86.15
Aedes albopictus	380	322	387	396	56	344	1,885	1,440 (776 females and 664 males)	76.39
Aedes aegypti	299	130	287	221	64	177	1,178	942 (442 females and 520 males)	79.97
TOTAL	**939**	**622**	**954**	**835**	**176**	**692**	**4,218**	**3,377 (1,712 females and 1,685 males)**	**80.06**

The reason of this valid recorded percentage was mainly because of two mosquitoes entered in the trap at the same time causing "double flights". Other reason was fan errors, causing "slow flights", hindering the correct detection of mosquitoes. Therefore, decrease the time needed between mosquito flights (actually 1 second), might improve the efficiency of the sensor. One the other hand, if the number of mosquitoes introduced in the box where the trap is allocated double flight could decrease.

Fundamental frequency of *Cx. pipiens*, *Ae. albopictus* and *Ae. aegipty*

The fundamental frequencies represent the wingbeat mosquito frequencies. The fundamental frequencies of each species obtained by the sensor are showed in Figure 2. Two peaks in each species are visualized in the histogram and they correspond to the sex peaks.

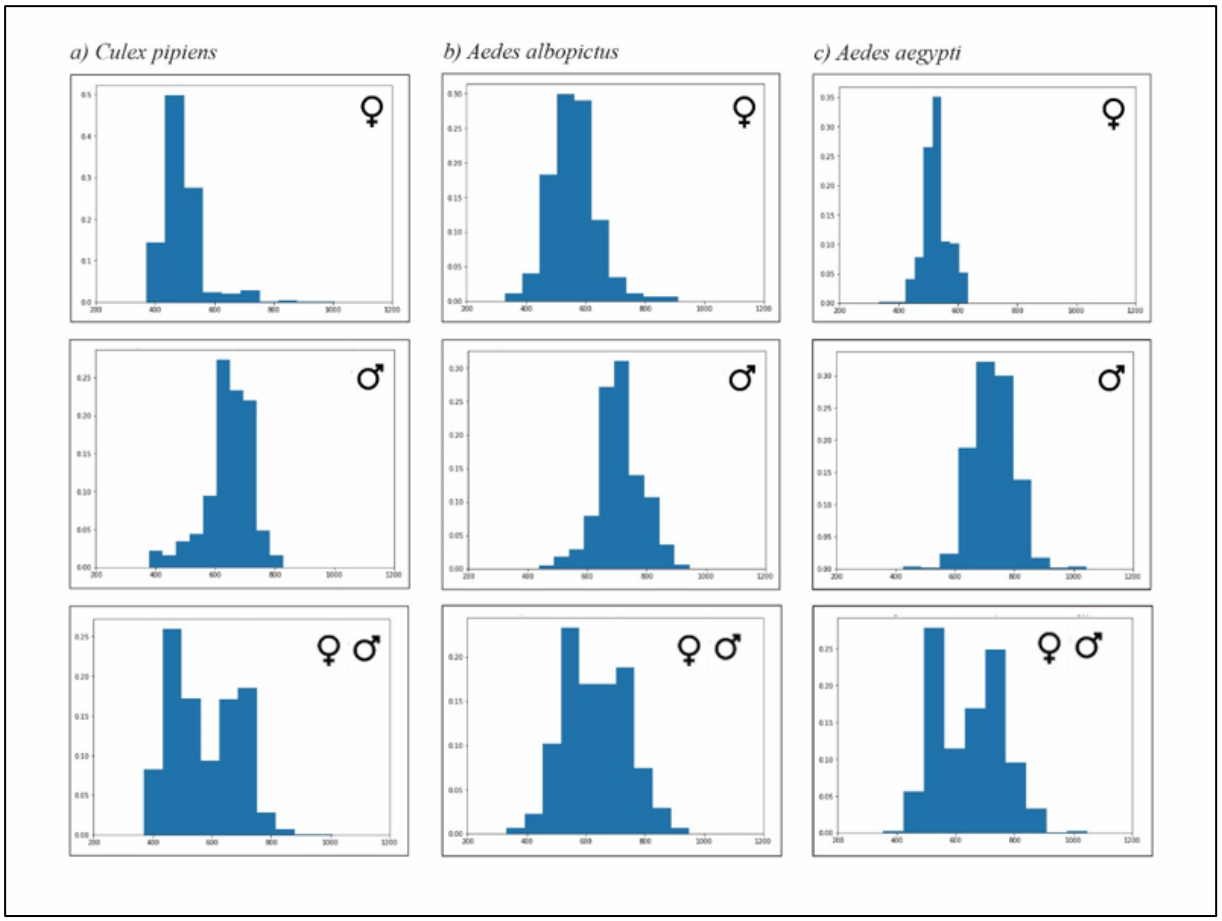

Figure 2, Fundamental frequency by sex. A) Cx. pipiens B) Ae. albopictus C) Ae. aegypti

The fundamental frequency histogram of species, sex and age showed that in all the age-points; 2-4 days (Figure 3), 7-8 days (Figure 4) and 14-16 days (Figure 5), the fundamental frequency by sex were always higher in males than in females but no differences have visually seen in fundamental frequency by age.

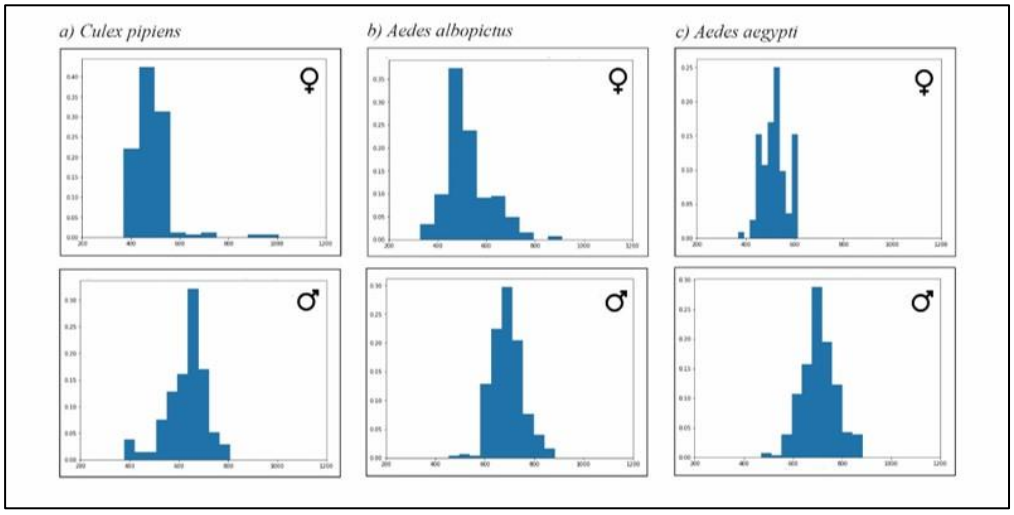

Figure 3, Fundamental frequency by age and sex (2-4 days) A) Cx. pipiens B) Ae. albopictus C) Ae. aegypti

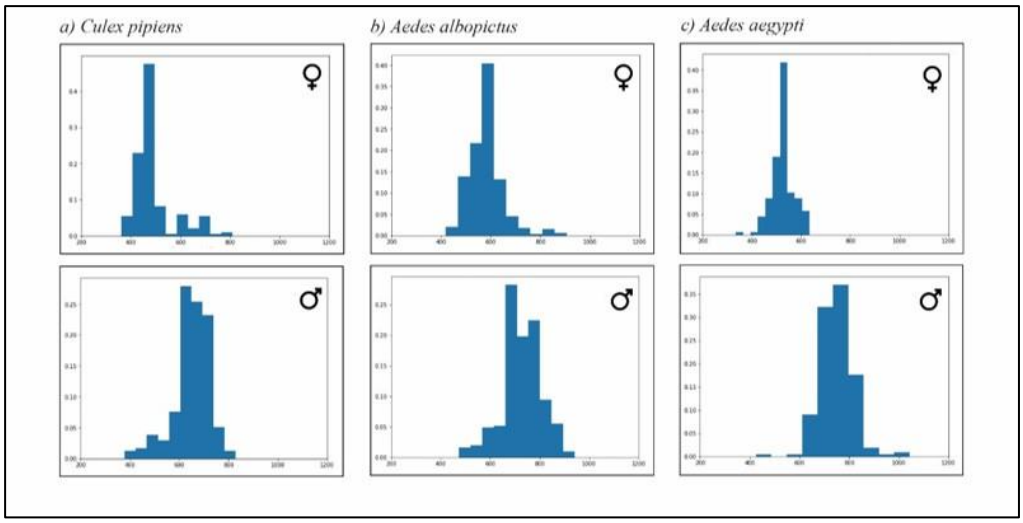

Figure 4, Fundamental frequency by age and sex (7-9 days) A) Cx. pipiens B) Ae. albopictus C) Ae. aegypti

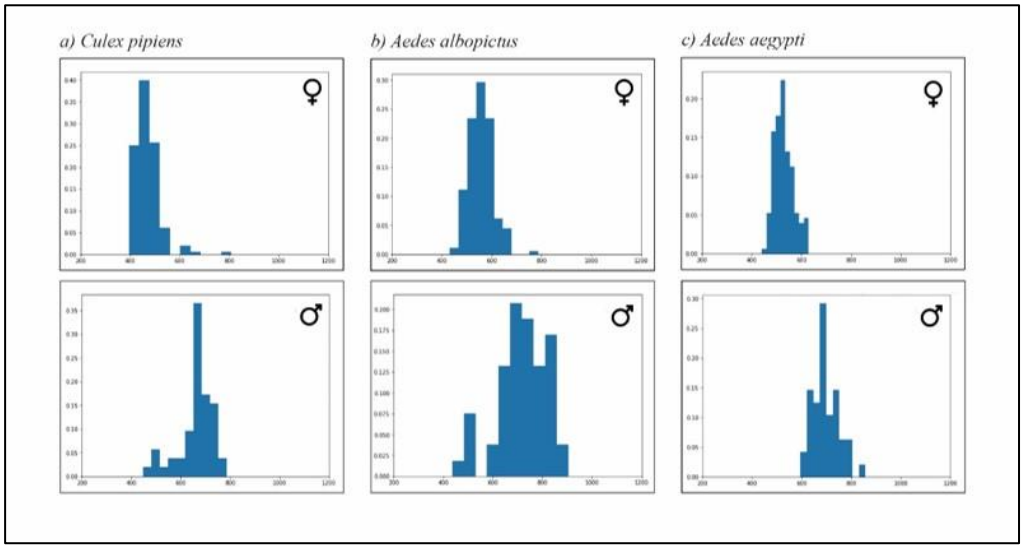

Figure 5, Fundamental frequency by age and sex (14-16 days) A) Cx. pipiens B) Ae. albopictus C) Ae. aegypti

Fundamental frequencies for specie and sex detected by the sensor are presented in Table 3. The values of fundamental frequency were not normal and showed statistical differences ($p<<0.05$) between females and males of each species. These results are in agreement with previous knowledge that males have high fundamental frequency that females for the same species (Clements, 1992). The wing beat fundamental frequency could be enough predictive variable to identify the gender of a mosquito as previously reported (Genoud *et al.*, 2018). Biologically, differences in wing shape between species for both males and females have been previously reported since all mosquito species have sexually dimorphic wings (Cator *et al.*, 2011).

Moreover, there were statistical differences in the mean fundamental frequencies of the female and male mosquitoes among the different species ($p<<0.05$). The results of the Dunn's test with Bonferroni correction indicate that all groups are statistically different from each other. *Culex pipiens* showed the lowest frequency followed by *Ae. aegipty* and *Ae. albopictus*, which had the highest frequency in our system where the ventilator was present. These results are in agreement with previous studied where the fundamental frequency was detected in free flight (Genoud *et al*., 2018).

Table 3, Mean fundamental frequency values by sex and specie

	Mean fundamental frequency (Hz)	
	♀	♂
Culex pipiens	457.240515	620.890075
Aedes albopictus	531.230713	684.221659
Aedes aegypti	508.986023	696.99659

An example of fundamental frequency in free flight at 18±1 ºC is: 344±7 for female and 541±7 for male of *Cx. pipiens*, 456±6 for female and 681±5 for male of *Ae. albopictus*, and 425±2 for female and 628±6 for male of *Ae. aegypti* (Genoud *et al.*, 2018). All the fundamental frequency values are lower than the obtained in the present study, which has been done at average temperature of 25.79ºC and RH of 52.13 % for *Cx. pipiens and Ae. albopictus* (BSL2 conditions) and at average temperature of 26.15ºC and RH of 51.88% for *Ae. aegypti* (BSL3 conditions). It has been seen that fundamental frequency is susceptible to temperature, increasing 8-13 Hz each ºC gain (Villareal, 2017), so this difference could be due to this factor. Other studies (Cator *et al*., 2011) in free flight at average temperature of 36.2ºC and RH of 59.9%, shows a fundamental frequency (Hz) of 664.3±4.6 for females and 982.0±1.0 for males of *Ae. aegypti* species. These results were higher values that those obtained in the present study. In practice, when a sensor such as the one in the present study is used in the field, different environmental factors should be considered, since, as can be seen, different temperatures affected the fundamental frequency.

In the Figure 6, the variations of fundamental frequency by age are shown. As the age of the mosquitoes progressed, the fundamental frequency increased until it became stable, like indicated previous free-flight reports (Clements, 1992).

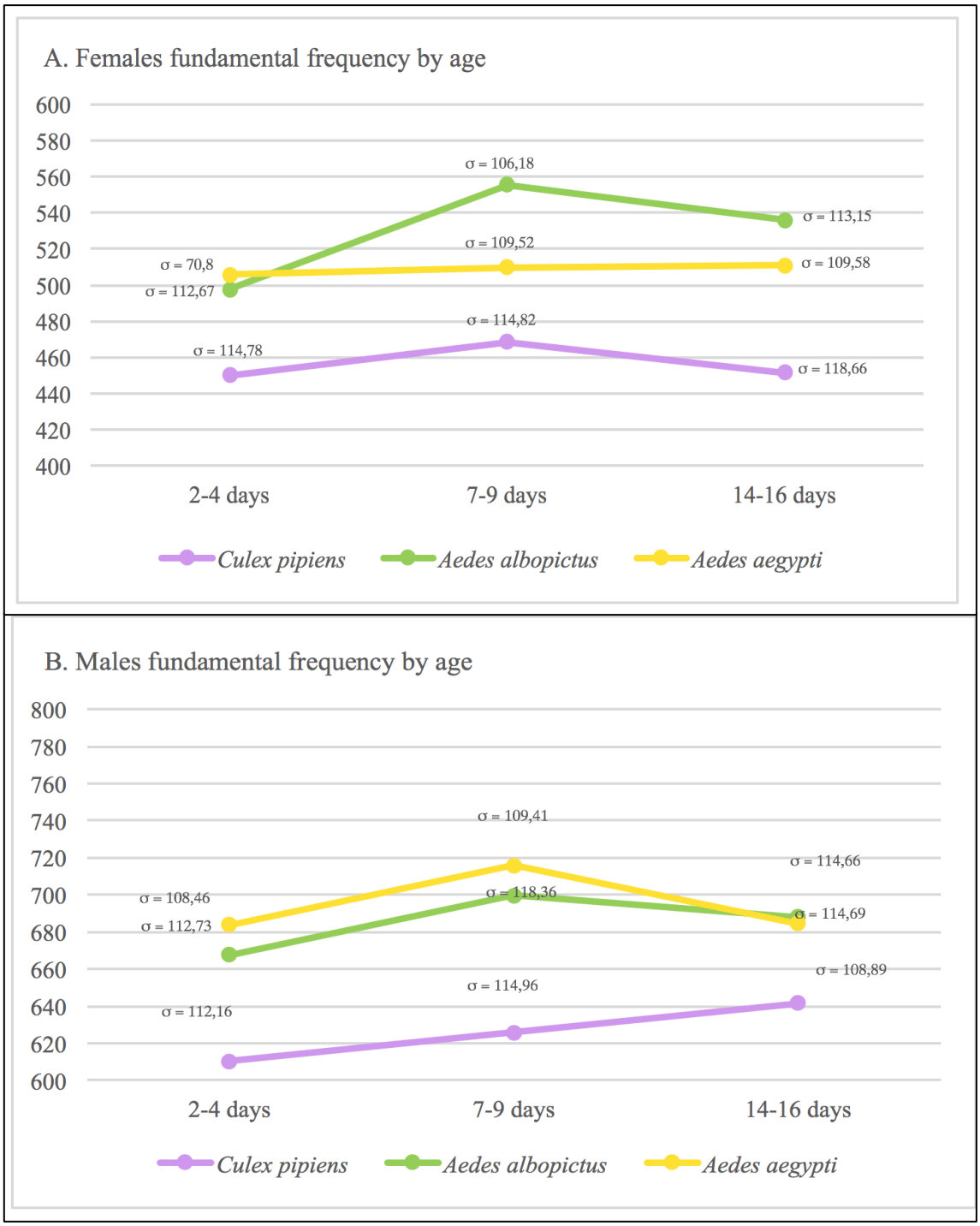

Figure 6, Fundamental frequency by species, sex and age. A) Females B) Males

Classification between species, sex and age by machine learning

For species, sex and age classification on the test set using machine learning 844 samples were used, which consisted in 25% of the number of available samples and had not been used during the training, which had used 2,533 samples.

Species classification

In this section the results of the species classification using machine learning are described. A machine learning process for all the combinations of species with two classes was performed.

Aedes albopictus and Culex pipiens

In the Table 4, the 3-best results of the classification between the species *Ae. albopictus* and *Cx. pipiens* are shown. The highest accuracy obtained was 93.83%.

Table 4, Results of species classification between Aedes albopictus and Culex pipiens

Characteristics used	**Number of features**	**Number of mosquito flight records***	**Algorithm**	**Accuracy**
Fresnel, Mel, peak amplitudes	70	972	XGBoost	93.83%
Harmonic form, Mel	70	972	XGBoost	93.01%
Fresnel, Mel	67	976	XGBoost	91.80%

** This is the size of the data set including train and test set. The best result is highlighted in green.*

The training and cross-validation score curves (Figure 7) indicated that with more data, the results could improve as there was a low bias but a high variance to achieve a highly successful classification between *Ae. albopictus* and *Cx. pipiens*.

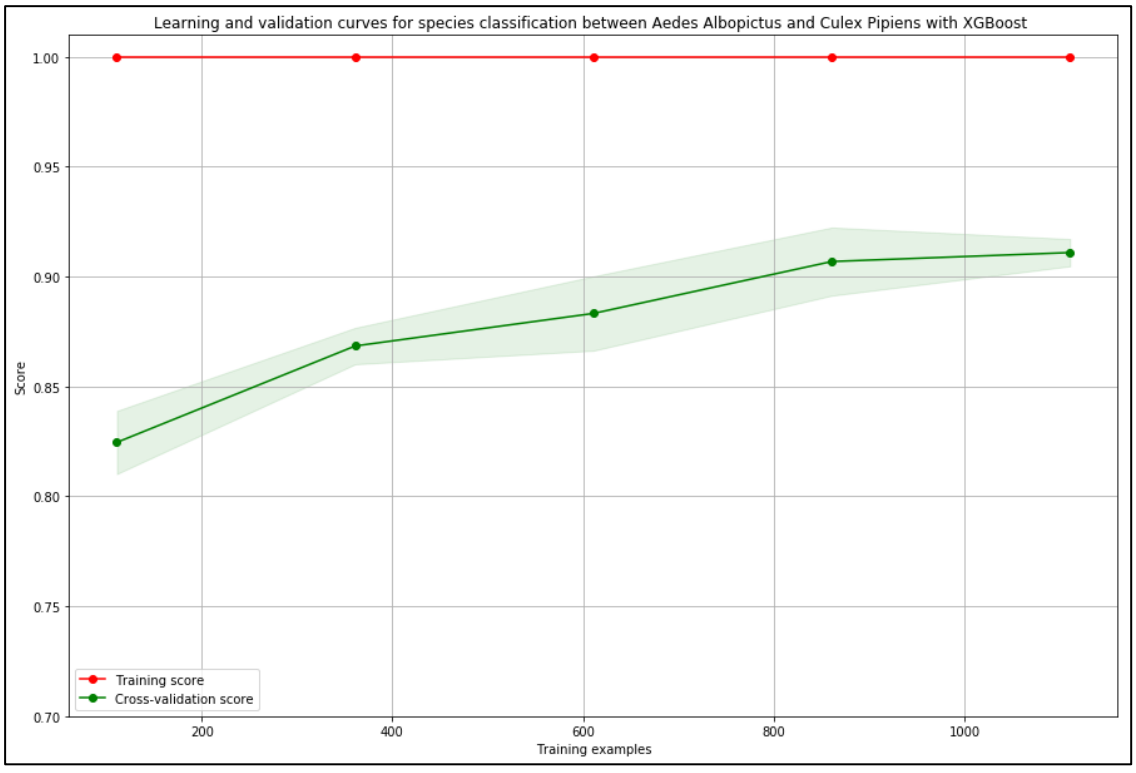

Figure 7, Learning and validation curves for species classification between Ae. albopictus and Cx. pipiens

Aedes aegypti and Culex pipiens

In the Table 5, the 3-best results of the classification between the species *Ae. aegypti* and *Cx. pipiens* are shown. The highest accuracy obtained was 95.73%.

Table 5, Results of species classification between Aedes albopictus and Culex pipiens

Characteristics used	**Number of features**	**Number of mosquito flight records***	**Algorithm**	**Accuracy**
Fresnel, harmonic frequencies, Mel, peak amplitudes,	73	1,688	Artificial neural network	95.73%
Fresnel, Mel, peak amplitudes	70	1,688	Artificial neural network	95.73%
Fresnel, Mel	67	1,688	Artificial neural network	95.49%

** This is the size of the data set including train and test set. The best result is highlighted in green.*

These were the high accuracy results between species classification and the learning and validation curves (Figure 8) indicated that more data could improve the results further as they have not converged yet. At this moment, the obtained results of accuracy are similar to those reported by Silva et al. (2015) who showed an accuracy of 95% for *Ae. aegypti* and is higher than the results obtained by Ouyang et al. (2015) who reported an accuracy of 88.1%.

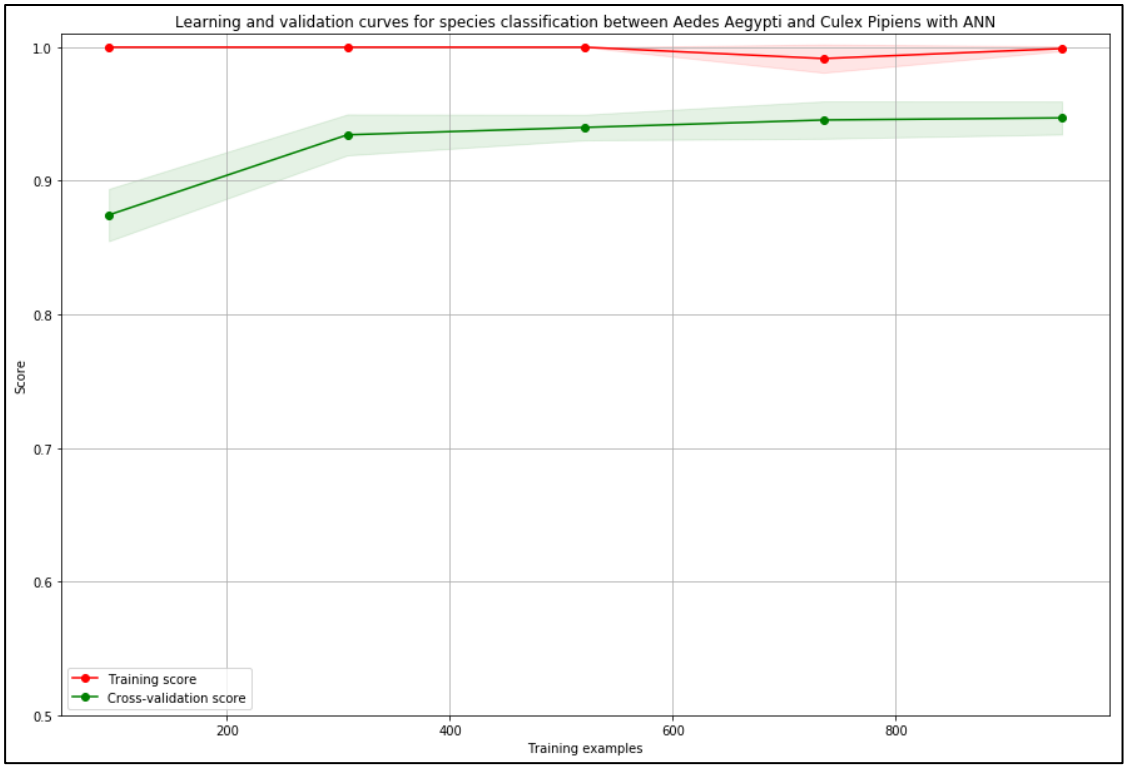

Figure 8, Learning and validation curves for species classification between Aedes Aegypti and Culex Pipiens

Aedes aegypti and Aedes albopictus

In the Table 6, the 3-best results of the classification between the species *Ae. aegypti* and *Ae. albopictus* are shown. The highest accuracy obtained was 76.06%.

Table 6, Results of species classification between Ae. aegypti and Ae. albopictus

Features used	**Number of features**	**Number of mosquito flight records***	**Algorithm**	**Accuracy**
Fresnel, harmonic forms, Mel	73	1,688	XGBoost	76.06%
Fresnel, Mel, peak amplitudes	70	1,688	Artificial Neural Network	76.06%
Fresnel, harmonic frequencies, harmonic powers, Mel	73	1,688	XGBoost	75.96%

** This is the size of the data set including train and test set.* The best result is highlighted in green.

The obtained scores in the training curve decreased with the number of training samples (Figure 9). However, it might be possible to differentiate the two species using the present model since the gap between learning curve and validation curve indicates that with more training data the results would improve.

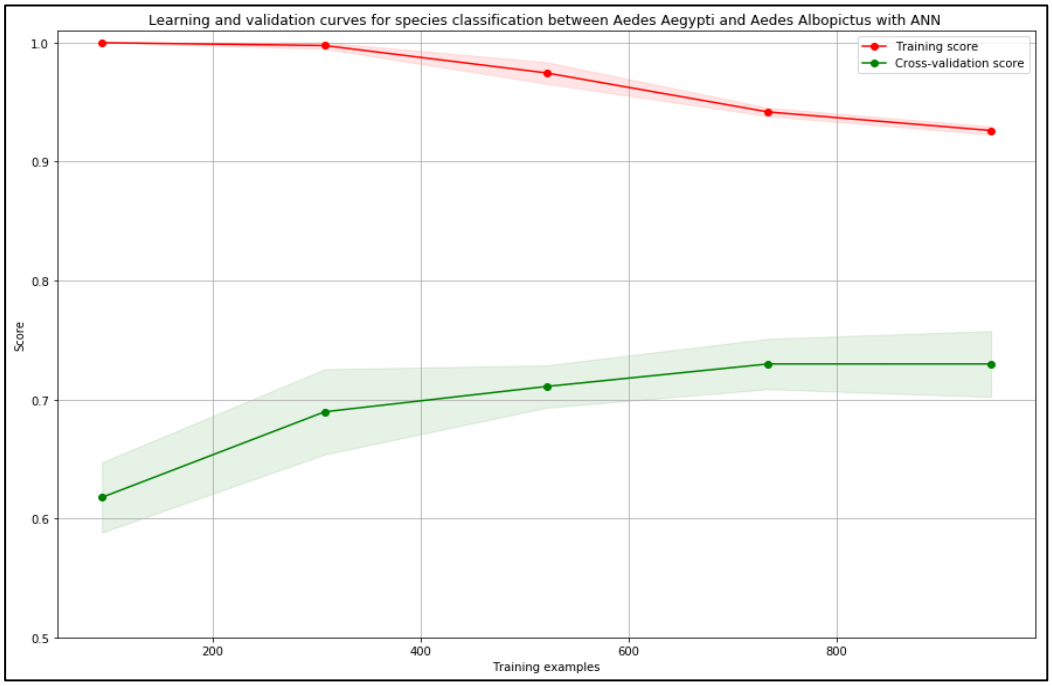

Figure 9, Learning and validation curves for species classification between Ae aegypti and Ae. albopictus

An entomologist can distinguish between *Culex* and *Aedes* genus practically without error due to their macroscopically visible biological differences. In this study, an accuracy of 93.83% between *Ae. albopictus* and *Cx. pipiens* and 95.73% between *Ae. aegypti* and *Cx. pipiens* have been shown. Instead, an accuracy of 76.07% between *Ae. albopictus* and *Ae. aegypti* showed, like previous results reported, that species in the same genus share similar wingbeat patterns, suggesting that the classification between two groups in the same genus would be challenging (Ouyang *et al.*, 2015).

Sex classification

A machine learning process was implemented for all the three species with the goal to distinguish between females and males.

Culex pipiens

In the Table 7, the 3-best results of the classification of *Cx. pipiens* into females and males are shown. The highest accuracy obtained was 93.11%.

Table 7, Results of sex classification of Cx. pipiens

Features used	**Number of features**	**Number of mosquito flight records***	**Algorithm**	**Accuracy**
Fresnel, harmonic form, Mel	73	988	XGBoost	93.11%
Harmonic form, Mel	70	988	XGBoost	93.11%
Fresnel, harmonic frequencies, Mel, peak amplitudes,	73	988	XGBoost	93.11%

** This is the size of the data set including train and test set. The best result is highlighted in green.*

These results were the lowest of all species for sex classification. Moreover, the learning and validation curves (Figure 10) indicated that in this moment it would not improve the results to have more training data as both curves have converged. It seems to be some laboratory errors and that some samples were labeled incorrectly in terms of sex. Therefore, to improve the results more *Cx. pipiens* should be reared to relabel correctly and retrain.

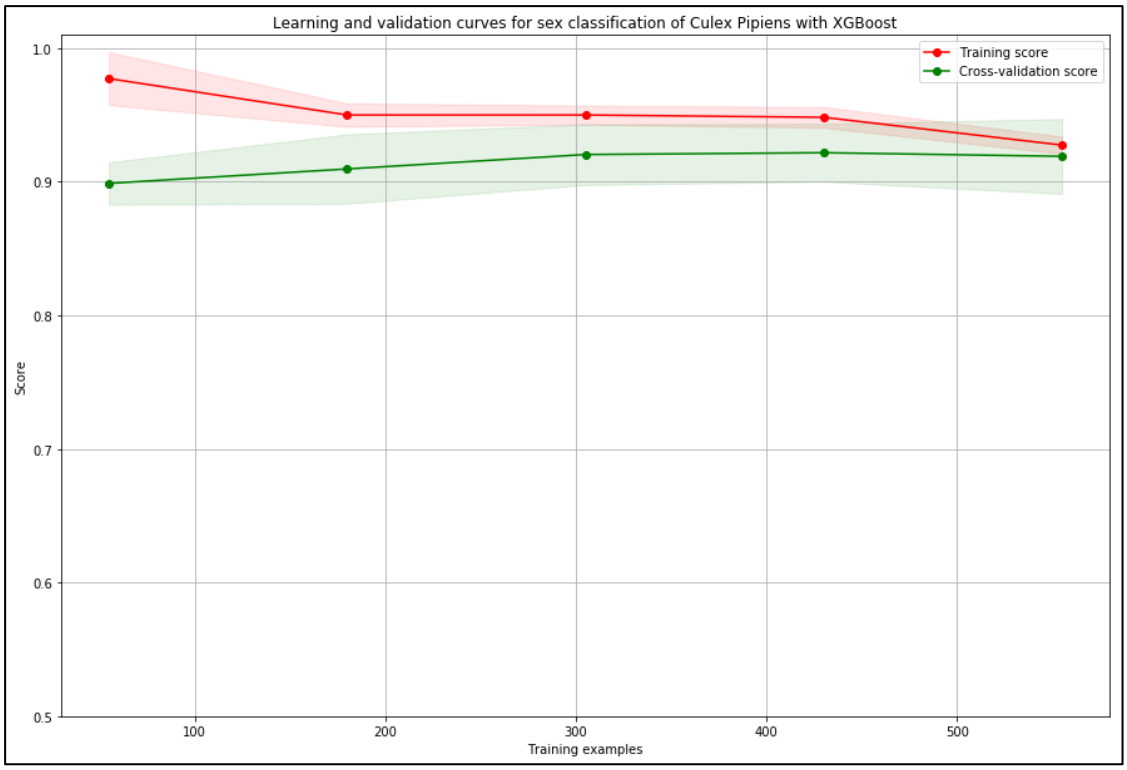

Figure 10, Learning and validation curves of sex classification of Cx. pipiens

Aedes albopictus

In the Table 8, the 3-best result of the classification of *Ae. albopictus* into females and males are shown. The highest accuracy obtained was 94.27%.

Table 8, Results of sex classification of Ae. albopictus

Features used	**Number of features**	**Number of mosquito flight records***	**Algorithm**	**Accuracy**
Fresnel, harmonic powers, Mel	70	1,328	Artificial neural network	94.27%
Fresnel, harmonic frequencies, harmonic powers, Mel	73	1,328	XGBoost	94.27%
Mel	64	1,328	XGBoost	93.97%

** This is the size of the data set including train and test set. The best result is highlighted in green.*

Females and males of *Ae. albopictus* (Figure 11A) are not as easily distinguishable as the sexes of *Ae. aegypti* (Figure 11B) since there is more overlapping in some features (fundamental

frequency and first peak amplitude). Consequently, we need a more complex model to obtain high scores.

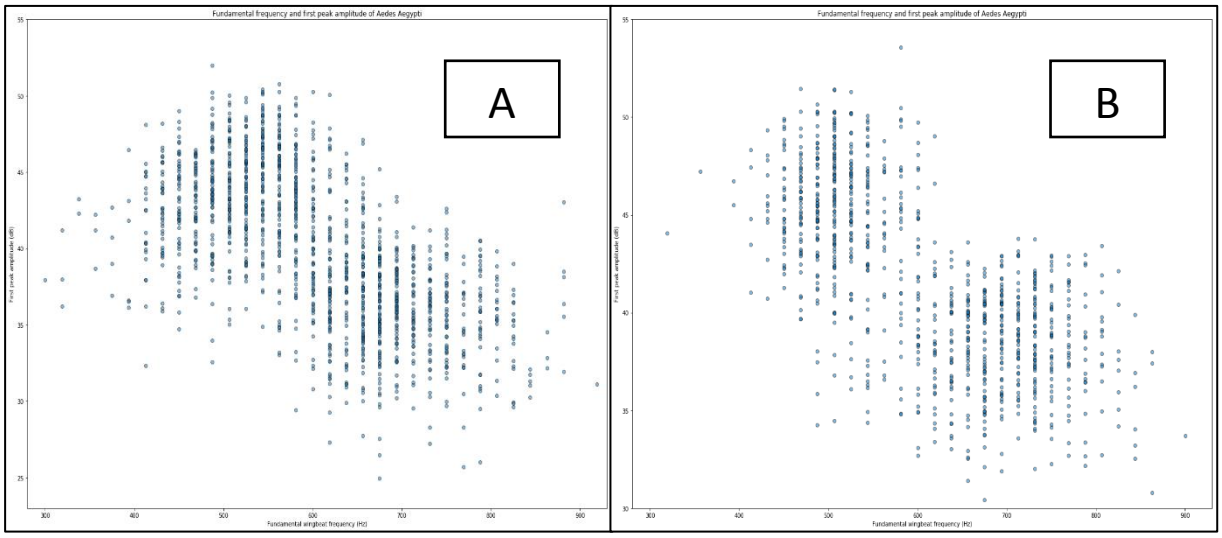

Figure 11, Scatter plot of fundamental frequency and first peak amplitude. A) Ae. albopictus B) Ae. aegypti.

Once more, the learning curves (Figure 12) indicated that more training could improve the results because of the low bias and high variance.

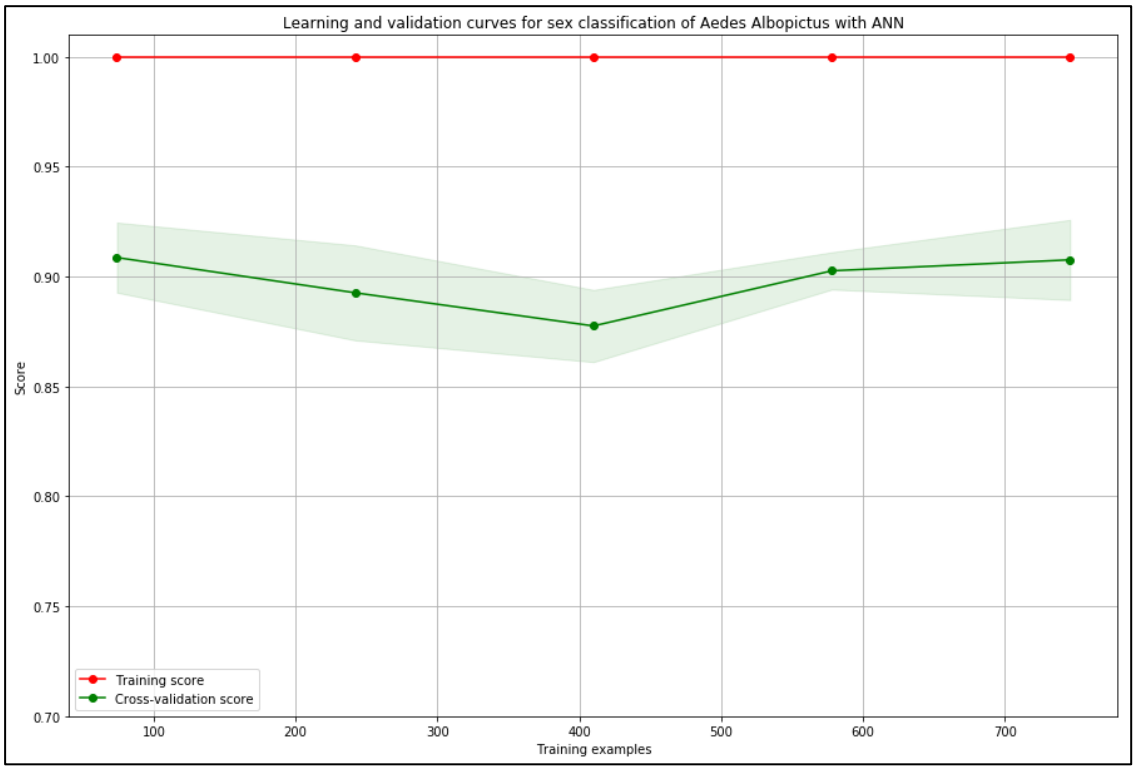

Figure 12, Learning and validation curves for sex classification of Ae. albopictus

Aedes aegypti

In the Table 9, the 3-best result of the classification of *Ae. aegypti* into females and males are shown. The highest accuracy obtained was 99.05%.

Table 9, Results of sex classification of Aedes aegypti

Features used	**Number of features**	**Number of mosquito flight records***	**Algorithm**	**Accuracy**
Fresnel, power spectral density without baseline, peak amplitudes	263	844	Artificial neural network	99.05%
Fresnel, harmonic powers	6	844	Support vector machines	99.05%
Fresnel, peak amplitudes, harmonic frequencies	9	844	Logistic regression	99.05%

** This is the size of the data set including train and test set. The best result is highlighted in green.*

The females and males of *Ae. aegypti* were easy to classify so that even a quite simple model obtains very high scores. Only 2 samples were wrongly classified by the present model. The learning and validation curves (Figure 13) indicated that with more training samples it would be possible improve the classification between sex of *Ae. aegypti*. As it was mentioned before, for *Ae. aegypti,* it is easier to visually differentiate with a fundamental frequency and first peak amplitude scatter plot (Figure 11B).

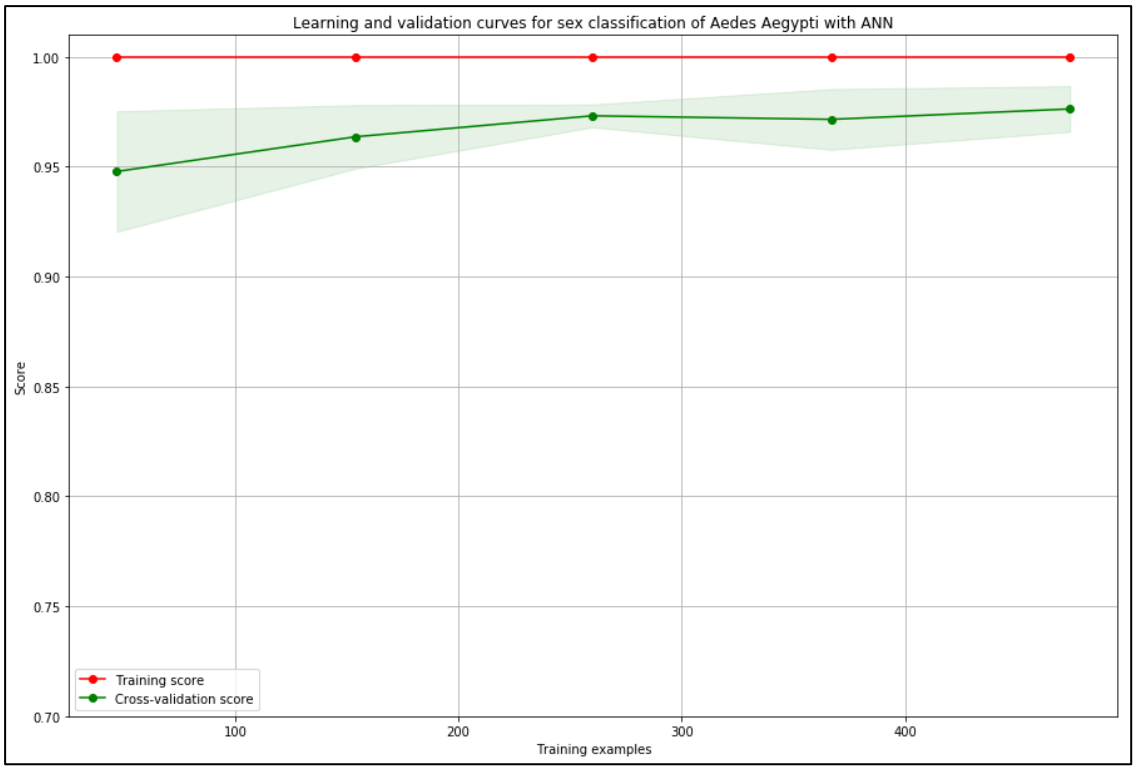

Figure 13, Learning and validation curves for sex classification of Ae. aegypti

Age classification

A machine learning process was implemented for both sexes of all the three species with the goal to distinguish between age-groups. Two age-groups were used for the classification: 2-4 days and 7-9 days. The specimens of 14-16 days were removed because there were less samples. The reason was that males do not tend to survive until this period.

Culex pipiens females

In the Table 10, the 3-best results of the classification of the age of the females of *Cx. pipiens* are shown. The highest accuracy obtained was 78.04%.

Table 10, Results of age classification for females of Cx. pipiens

Features used	Number of features	Number of mosquito flight records*	Algorithm	Accuracy
Fresnel, Mel	67	326	Artificial Neural Network	78.04%
Fresnel, harmonic frequencies,Mel, peak amplitude	73	326	XGBoost	76.74%
Fresnel, harmonic forms, Mel	73	326	Artificial Neural Network	75.60%

** This is the size of the data set including train and test set. The best result is highlighted in green.*

These results and the learning and validation curves (Figure 14) indicate that with more training samples it would be possible to successfully classify females of *Cx. pipiens* into age groups.

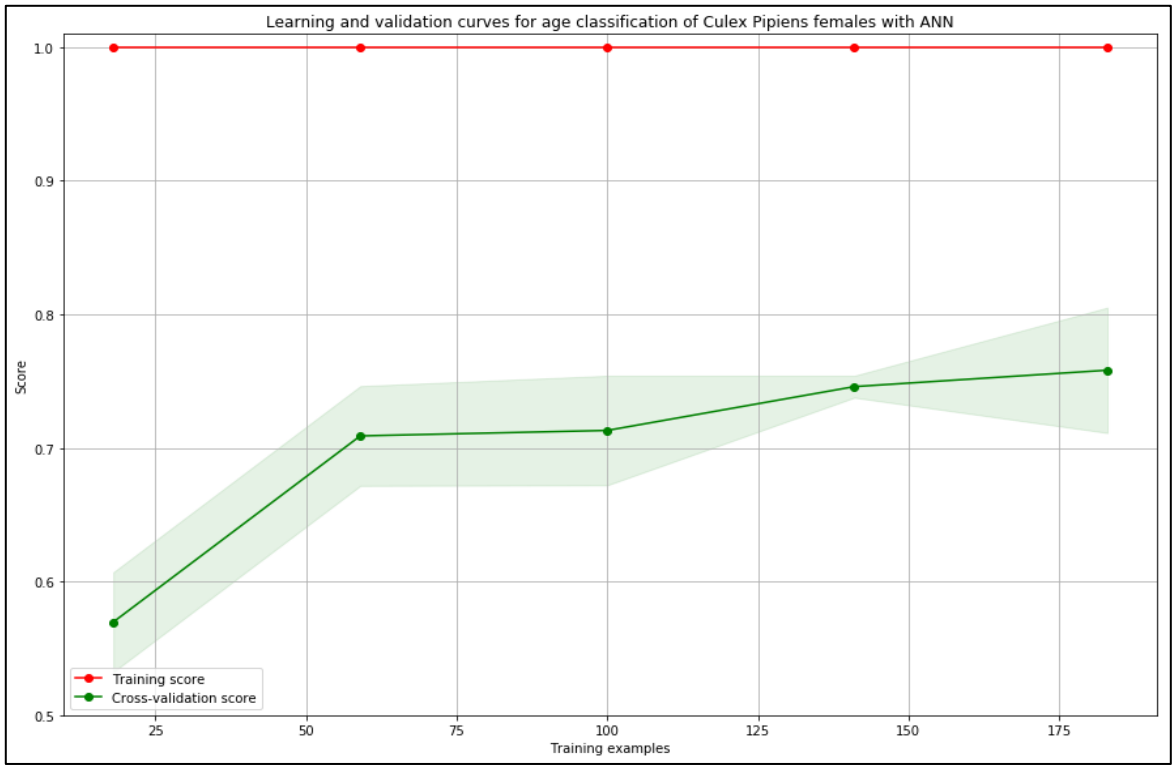

Figure 14, Learning and validation curves of age classification for females of Cx. pipiens

Culex pipiens males

In the Table 11, the 3-best results of the classification of the age of the males of *Cx. pipiens* are shown. The highest accuracy obtained was 69.81%.

Table 11, Results of age classification for males of Culex Pipiens

Features used	**Number of features**	**Number of mosquito flight records***	**Algorithm**	**Accuracy**
Fresnel, harmonic frequencies, harmonic powers, Mel	73	424	XGBoost	69.8113%
Fresnel, harmonic frequencies Mel, peak amplitudes,	73	424	XGBoost	67.9245%
Harmonic powers, Mel, PSD	324	424	XGBoost	66.9811%

** This is the size of the data set including train and test set. The best result is highlighted in green.*

These were the results with lower accuracy. Once more, with more samples they are worse than those of females of *Cx. pipiens* indicating that males are more difficult to classify. The learning and validation curves (Figure 15215) indicate that with more training data the results would improve because the curves have not converged.

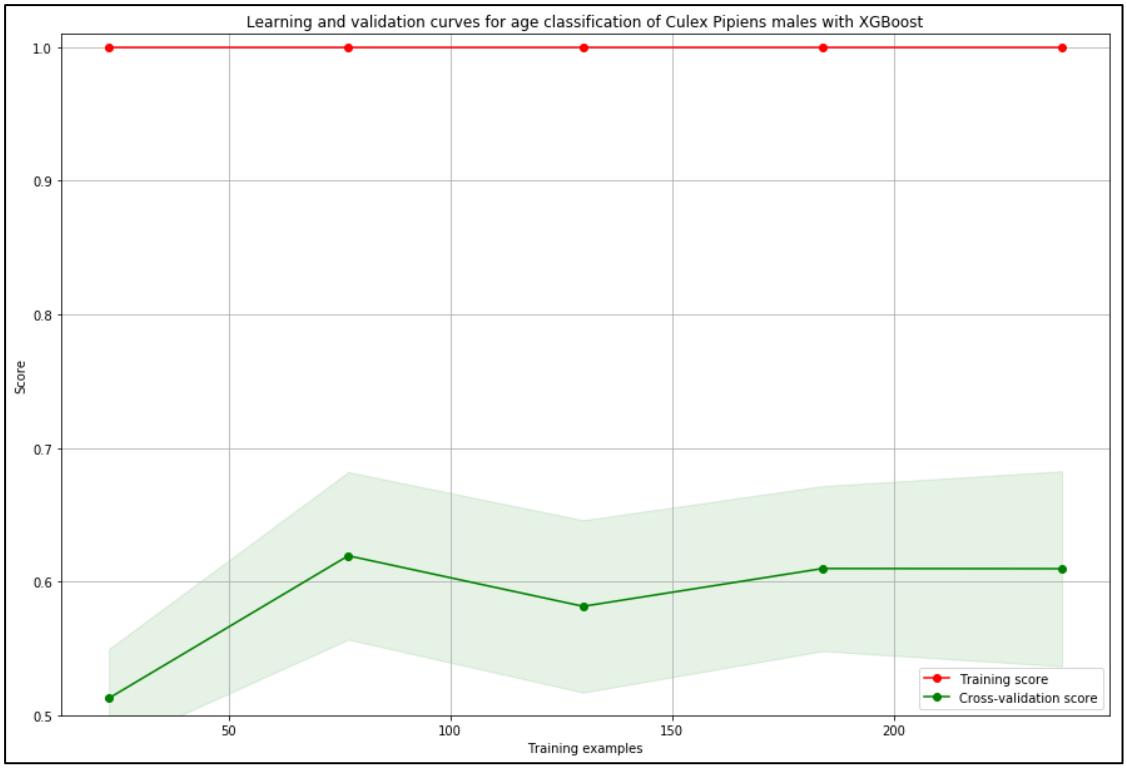

Figure 152, Learning and validation curves for age classification of males of Culex Pipiens

Aedes albopictus females

In the Table 12, the 3-best results of the classification of the age of the females of *Ae. albopictus* are shown. The highest accuracy obtained was 90.97%.

Table 12, Results of age classification for females of Ae. albopictus

Features used	**Number of features**	**Number of mosquito flight records***	**Algorithm**	**Accuracy**
Fresnel, MFCC	67	530	Artificial neural network	90.97%
MFCC, power spectral density, peak amplitudes	324	530	XGBoost	90.97%
harmonic powers, MFCC, power spectral density	324	530	XGBoost	90.97%

** This is the size of the data set including train and test set. The best result is highlighted in green.*

The obtained results were interesting considering the small amount of training data available. Furthermore, the learning and validation curves (Figure 16) indicated that with more data the results could improve as learning curve and validation curve have not converged using the maximum of available training examples.

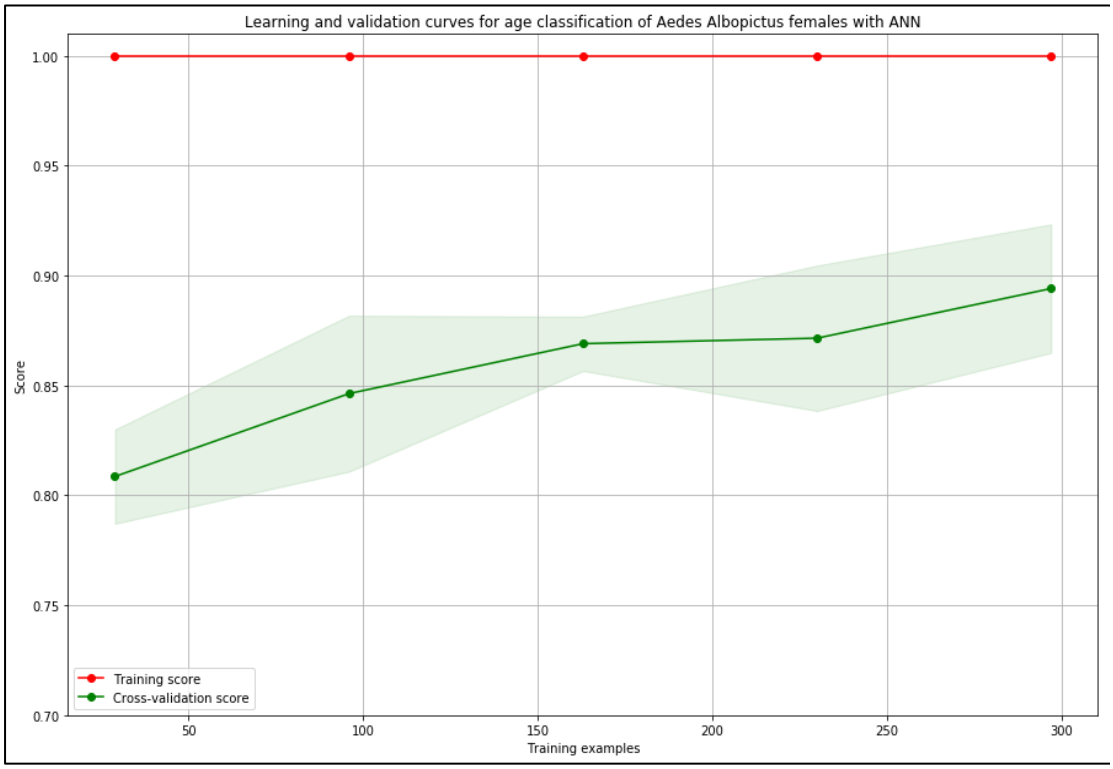

Figure 16, Learning and validation curves of age classification for females of Ae. albopictus

Aedes albopictus males

In the Table 13, the 3-best results of the classification of the age of the males of *Ae. albopictus* are shown. The highest accuracy obtained was 86.84%.

Table 13, Results of age classification for males of Ae. albopictus

Features used	**Number of features**	**Number of mosquito flight records***	**Algorithm**	**Accuracy**
Fresnel, harmonic frequencies, harmonic powers, MFCC	73	606	Artificial neural network	86.84%
MFCC, harmonic powers, power spectral density	324	606	XGBoost	86.18%
Fresnel, harmonic frequencies,MFCC, peak amplitudes	73	606	Artificial neural network	85.52%

** This is the size of the data set including train and test set. The best result is highlighted in green.*

These results were also quite good for the small amount of training data and indicated that is possible to classify the males of *Ae. albopictus* into age groups. Having more data of males than for females but worse results might be an indication that the females are easier to classify into age groups with these methods. In the Figure 17, the validation curve indicated that more data would improve the results.

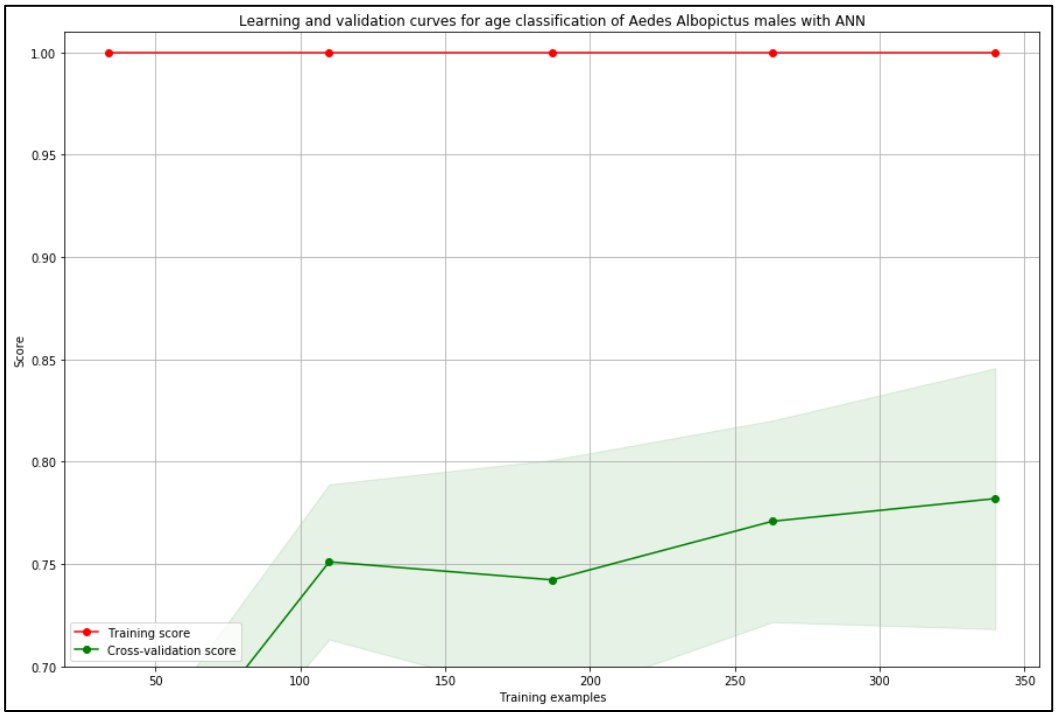

Figure 17, Learning and validation curves of age classification for males of Ae. albopictus

Aedes aegypti females

In the Table 14, the 3-best results of the classification of the age of the females of *Ae. aegypti* are shown. The highest accuracy obtained was 71.42%.

Table 14: Results of age classification for females of Ae. aegypti

Features used	**Number of features**	**Number of mosquito flight records***	**Algorithm**	**Accuracy**
Fresnel, MFCC	67	224	Artificial Neural Network	71.42%
Fresnel, harmonic form, MFCC	73	224	XGBoost	71.42%
Fresnel, harmonic frequencies, MFCC, peak amplitudes	73	224	XGBoost	71.42%

** This is the size of the data set including train and test set. The best result is highlighted in green.*

The obtained results were not very good, but the training data set was also very small and the learning and validation curves (Figure 18) indicated that more data would improve the results because learning and validation curve have not converged.

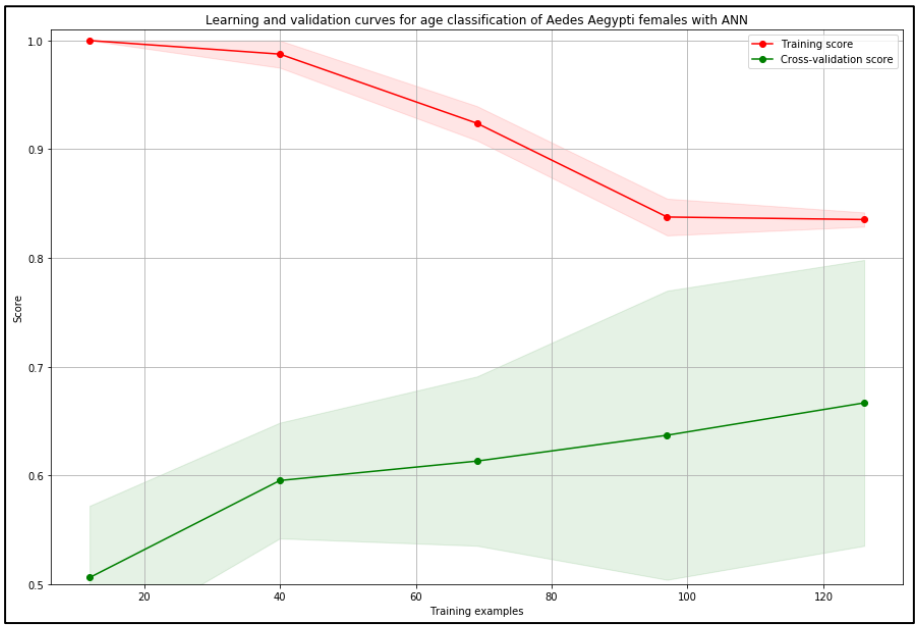

Figure 18, Learning and validation curves of age classification for females of Aedes aegypti

Aedes aegypti males

In the Table 15, the 3-best results of the classification of the age of the males of *Ae. aegypti* are shown. The highest accuracy obtained was 70.75%.

Table15, Results of age classification for males of Ae. aegypti

Features used	**Number of features**	**Number of mosquito flight records***	**Algorithm**	**Accuracy**
Fresnel, harmonic frequencies, Mel, peak amplitudes	73	422	XGBoost	70.75%
Mel	64	422	Artificial Neural Network	67.92%
Harmonic forms, Mel, total power	71	422	XGBoost	67.92%

** This is the size of the data set including train and test set. The best result is highlighted in green.*

The obtained results were worse than for the females with almost the double amount of training data available. As with *Cx. pipiens* and *Ae. albopictus,* this might be an indication that, with these methods, males are more difficult to classify into age groups, like learning and validation curves shown (Figure 19).

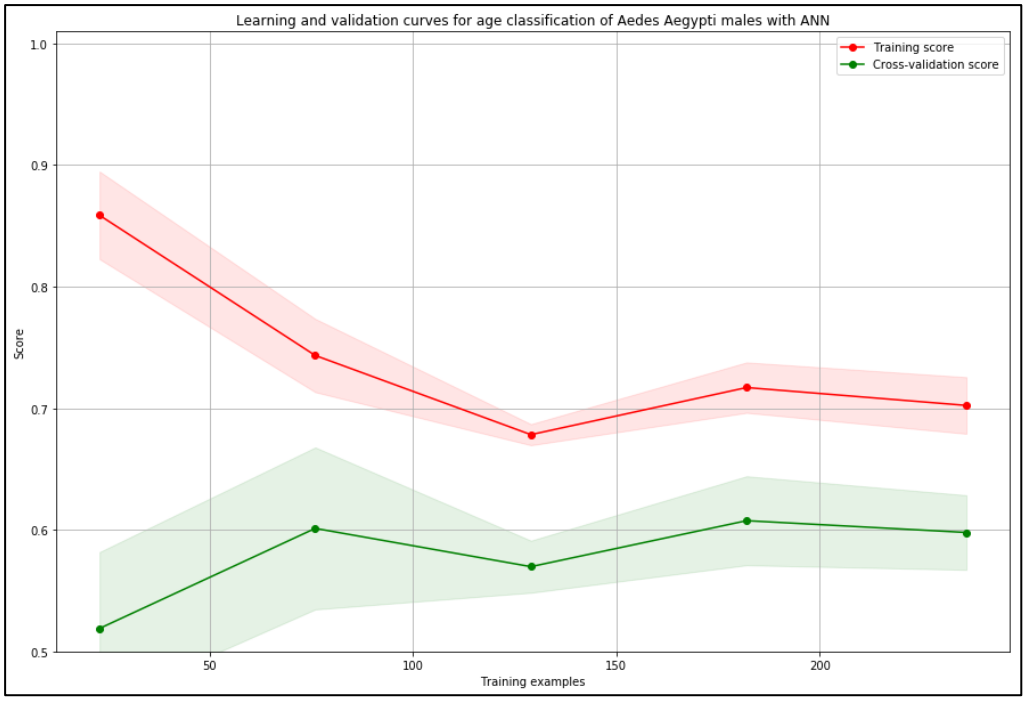

Figure 19, Learning and validation curves of age classification for males of Aedes aegypti

Entomologists can distinguish gender of a specie visually in the field, due to the biological differences in body size, maxillary palps and antennae, but they have to do very laborious dissections to estimate their physiological age, and age is an important factor in the vector capacity of mosquitoes, the older they are, the grater possibility of being infected and vector (Novoseltsev *et al*., 2012). In this study, more accuracy for the age classification of females have been seen than in males. This is advantageous in a surveillance plan because females are the important one of arbovirus transmissions.

Conclusions

- For the first time, an optical sensor connected in an air-forced trap has been evaluated and machine learning used for mosquito species, sex and age evaluation.
- In this study, the results obtained with an optical sensor connected in an air-forced trap were significant and capable to distinguish between species and sex in terms of fundamental frequency showing that the fundament frequency was higher in males than females and higher in mosquitoes of *Aedes* than in *Culex* genus.
- The system proposed in this study is advantageous because of its superior accuracy on genus classification compared with other optical sensors. More data and training is necessary to optimize the sensor to better classify mosquito species of the same genus.
- In the case of gender identification, male and female were discriminated with more than 93.11% of accuracy. This information will be important for arbovirus surveillance programs since the females are the unique implied in arbovirus transmission.
- It has been possible, for the first time, to classify mosquitoes according to ages with a range accuracy from 69.81% to 90.97% using machine learning and an optical sensor connected in an air-forced trap. This data might allow to know how old the mosquito population is and it would provide data useful for risk assessment due to the importance of the age in vector capacity.
- More biological (body size, females gonotrophic status) and ecological variables (environmental conditions) should be analyzed to increase the variance of the estimated mosquito model and validate it in the field so that optimize this novel optical sensor connected in a mosquito trap in order to improve mosquito vector surveillance.

Annex I

Extracted features

- MFCC: The MFCC of the audio signal. It was generated with 32 mel frequency bands (Zheng *et al*., 2001). Number of features: 32.
- Mel-scaled spectrogram: The mel-scaled spectrogram of the audio signal. Number of features: 32.
- PSD and PSD without baseline: The power spectral density of the waveform describes the power present in the signal as a function of frequency, per unit frequency [Hz] (Figure A). It has been generated using the python signal processing library scipy.signal with a Hanning window, a segment length of 512 points and an overlapping of 256 points. The Power spectral density without baseline is the whole estimate of the power spectral density generated the same way as described above but with the baseline subtracted (Martin, 2001). Number of features: 257 each.

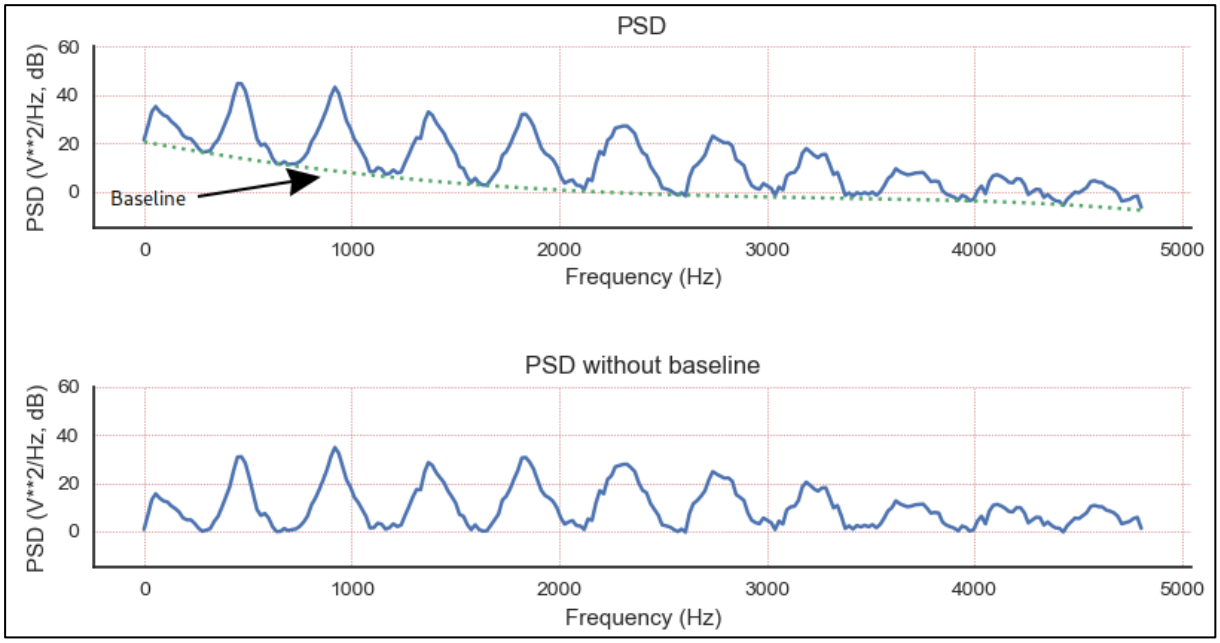

Figure A, PSD with and without baseline

- First harmonic power: the integrated power under of the first harmonic peak expressed in dB (Figure B). The first harmonic power is marked as a green area. Second and third harmonic power are also extracted features. Number of features: 1 each.

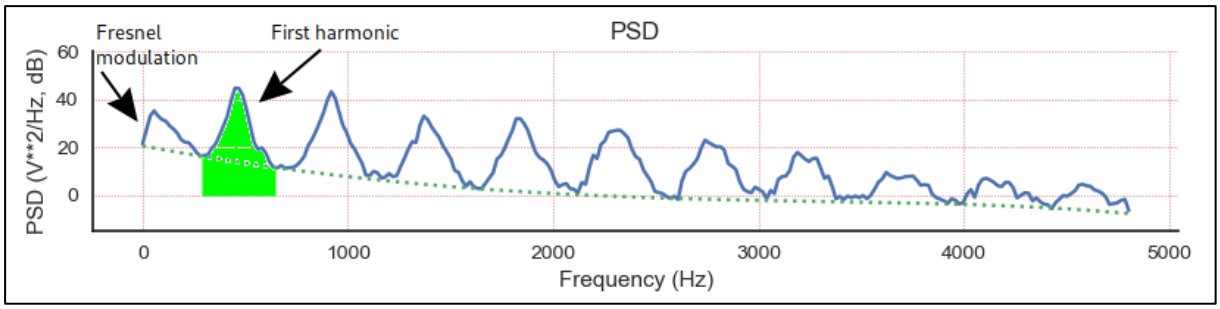

Figure B, First harmonic power: the green area marks the first harmonic power.

- First harmonic start and length: The number of the value of the PSD at which the first harmonic begins. If we have, for example, a record of 976 samples and the estimate of the power spectral density would have a length of 257 the first harmonic start might be at the sample number 16. First harmonic length is the width of the base of the first harmonic expressed in the number of points of the PSD (Figure C). Second and third harmonic start and length are also extracted features. Number of features: 1 each.

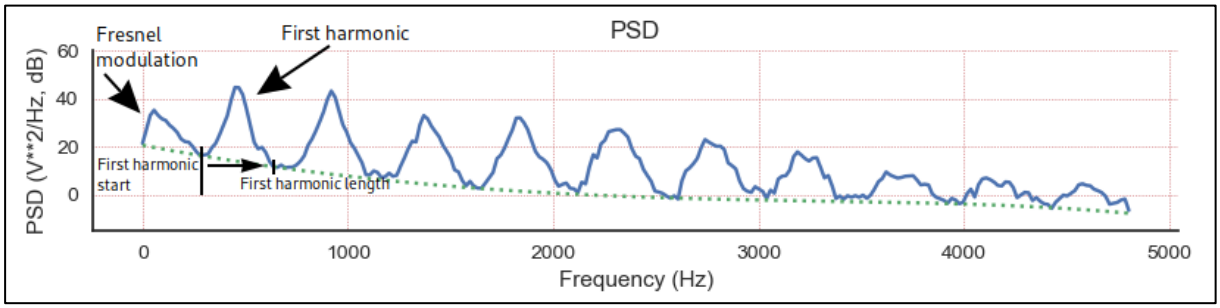

Figure C, First harmonic start and length

- First peak amplitude: The maximum PSD amplitude of the first harmonic expressed in dB (Figure D). Second and third peak amplitude are also extracted features. Number of features: 1 each.

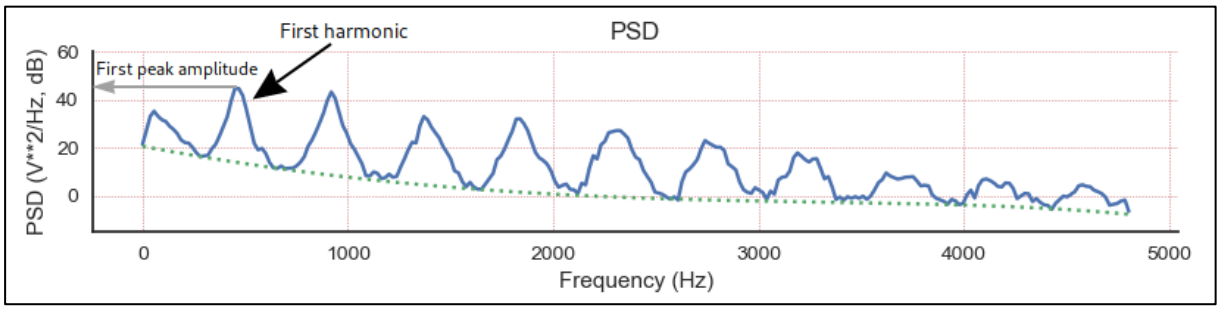

Figure D, First peak amplitude

- Fundamental frequency: The frequency of the peak of the first harmonic expressed in Hz (Figure E). Second and third harmonic frequency are also extracted features. Number of features: 1 each.

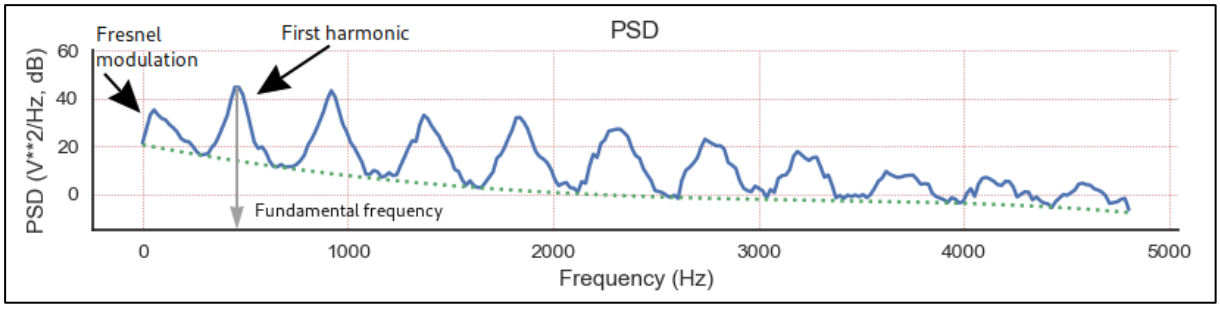

Figure E, Fundamental frequency

- Fresnel amplitude, frequency and power: The maximum PSD amplitude, in dB, of the low frequency peak to the left of the first harmonic (Figure F). The so called "Fresnel modulation" arises because the light intensity across the surface of the 2D sensor is not perfectly uniform. As the mosquito flies down through the sensor, it passes through 4 intense light regions, each with a less intense region above and below. This gives rise to amplitude modulation of the time domain signal, which is then reflected in the PSD plot. Fresnel amplitude is larger for mosquitoes with larger bodies. It is also larger for flights with faster transit times, because the response of the sensor falls by around 12 dB per octave below 300 Hz approximately.

  The Fresnel frequency is the frequency of the Fresnel modulation. With a typical transit time of 50 ms, the modulation frequency is 80 Hz.

  The Fresnel power, in dB, is the integrated power under the Fresnel modulation peak. Number of features: 1 each.

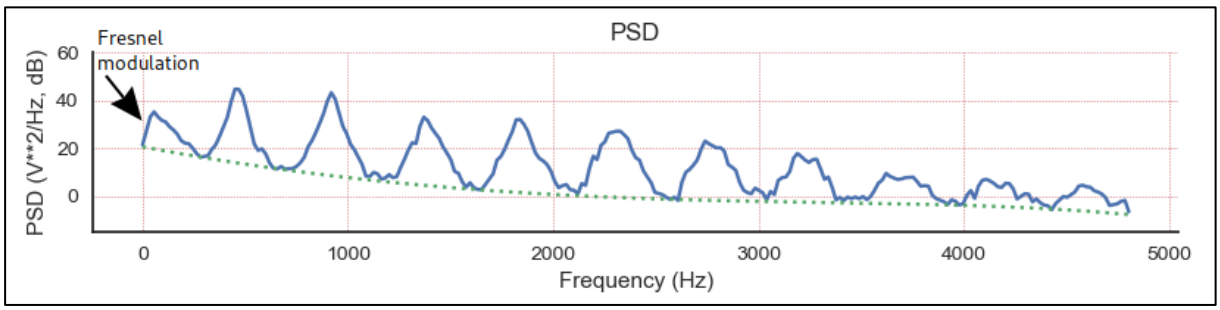

Figure F, Fresnel modulation

- Standard deviation: The standard deviation of the estimate of the power spectral density expressed in dB rms. Number of features: 1.

- Standard deviation without baseline is the standard deviation of the estimate of the power spectral density with the baseline subtracted expressed in dB rms. Number of features: 1.
- Total power: The total power of the estimate of the power spectral density expressed in dB (Figure G). The green area marks the total power. Number of features: 1.

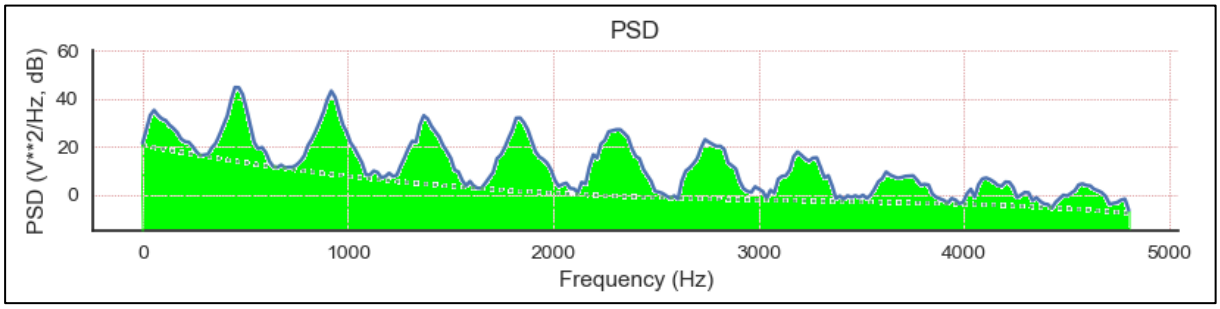

Figure G, Total power: The green area marks the total power.

- Total power without baseline: The total power of the estimate of the power spectral density with the baseline subtracted expressed in dB. Number of features: 1.

REFERENCES

Amraoui, F., Vazeille, M., & Failloux, A. B. (2016). French *Aedes albopictus* are able to transmit yellow fever virus. Eurosurveillance, 21(39).

Arthur, B. J., Emr, K. S., Wyttenbach, R. A., & Hoy, R. R. (2014). Mosquito (*Aedes aegypti*) flight tones: Frequency, harmonicity, spherical spreading, and phase relationships. The Journal of the Acoustical Society of America, 135(2), 933-941.

Becker, N., Petrić, D., Boase, C., Lane, J., Zgomba, M., Dahl, C., & Kaiser, A. (2003). Mosquitoes and their control (Vol. 2). New York: Springer.

Brady, O. J., Johansson, M. A., Guerra, C. A., Bhatt, S., Golding, N., Pigott, D. M., ... & Styer, L. M. (2013). Modelling adult *Aedes aegypti* and *Aedes albopictus* survival at different temperatures in laboratory and field settings. Parasites & vectors, 6(1), 351.

Brogdon, W. G. (1994). Measurement of flight tone differences between female *Aedes aegypti* and *Ae. albopictus* (Diptera: Culicidae). Journal of medical entomology, 31(5), 700-703.

Brustolin, M., Talavera, S., Santamaría, C., Rivas, R., Pujol, N., Aranda, C., ... & Busquets, N. (2016). Culex pipiens and Stegomyia albopicta (= *Aedes albopictus*) populations as vectors for lineage 1 and 2 West Nile virus in Europe. Medical and veterinary entomology, 30(2), 166-173.

Brustolin, M., Talavera, S., Nuñez, A., Santamaría, C., Rivas, R., Pujol, N., ... & Busquets, N. (2017). Rift V alley fever virus and E uropean mosquitoes: vector competence of *Culex pipiens* and Stegomyia albopicta (= *Aedes albopictus*). Medical and veterinary entomology, 31(4), 365-372.

Byrne, K., & Nichols, R. A. (1999). Culex pipiens in London Underground tunnels: differentiation between surface and subterranean populations. Heredity, 82(1), 7

Caputo, B., Ienco, A., Cianci, D., Pombi, M., Petrarca, V., Baseggio, A., ... & Della Torre, A. (2012). The "auto-dissemination" approach: a novel concept to fight *Aedes albopictus* in urban areas. PLoS neglected tropical diseases, 6(8), e1793.

Cator, L. J., Arthur, B. J., Ponlawat, A., & Harrington, L. C. (2011). Behavioral observations and sound recordings of free-flight mating swarms of *Ae. aegypti* (Diptera: Culicidae) in Thailand. Journal of medical entomology, 48(4), 941-946.

Clements, A. N. (1992). The biology of mosquitoes.

European Centre for Disease Prevention and Control. (2012). Guidelines for the surveillance of invasive mosquitoes in Europe. Retrieved from https://ecdc.europa.eu/sites/portal/files/media/en/publications/Publications/TER-Mosquito-surveillance-guidelines.pdf

European Centre for Disease Prevention and Control. (2014). Guidelines for the surveillance of native mosquitoes in Europe. Technical report. Retrieved from https://ecdc.europa.eu/sites/portal/files/media/en/publications/Publications/surveillance-of%20native-mosquitoes%20-guidelines.pdf

European Centre for Disease Prevention and Control and European Food Safety Authority. (2018). Mosquito maps. Retrieved from https://ecdc.europa.eu/en/disease-vectors/surveillance-and-disease-data/mosquito-maps

Farajollahi, A., Fonseca, D. M., Kramer, L. D., & Kilpatrick, A. M. (2011). "Bird biting" mosquitoes and human disease: a review of the role of *Culex pipiens* complex mosquitoes in epidemiology. Infection, genetics and evolution, 11(7), 1577-1585.

Flores, C. (2015). Mosquito Surveillance for Effective Mosquito Population Control International. Vector Disease Control. Retrieved from http://www.vdci.net/blog/mosquito-surveillance-for-effective-mosquito-population-control

Genoud, A. P., Basistyy, R., Williams, G. M., & Thomas, B. P. (2018). Optical remote sensing for monitoring flying mosquitoes, gender identification and discussion on species identification. Applied Physics B, 124(3), 46.

Gibson, G., Warren, B., & Russell, I. J. (2010). Humming in tune: sex and species recognition by mosquitoes on the wing. Journal of the Association for Research in Otolaryngology, 11(4), 527-540.

Iams, S. M. (2012). Free flight of the mosquito *Aedes aegypti*. arXiv preprint arXiv:1205.5260.

Kilpatrick, A. M., Meola, M. A., Moudy, R. M., & Kramer, L. D. (2008). Temperature, viral genetics, and the transmission of West Nile virus by *Culex pipiens* mosquitoes. PLoS pathogens, 4(6), e1000092.

Kraemer, M. U., Sinka, M. E., Duda, K. A., Mylne, A. Q., Shearer, F. M., Barker, C. M., ... & Hendrickx, G. (2015). The global distribution of the arbovirus vectors *Aedes aegypti* and *Ae. albopictus*. elife, 4

Lee, S. H., Nam, K. W., Jeong, J. Y., Yoo, S. J., Koh, Y. S., Lee, S., ... & Lee, K. H. (2013). The effects of climate change and globalization on mosquito vectors: evidence from Jeju Island, South Korea on the potential for Asian tiger mosquito (*Aedes albopictus*) influxes and survival from Vietnam rather than Japan. PloS one, 8(7), e68512.

Martin, R. (2001). Noise power spectral density estimation based on optimal smoothing and minimum statistics. IEEE Transactions on speech and audio processing, 9(5), 504-512.

Medlock, J. M., Snow, K. R., & Leach, S. (2005). Potential transmission of West Nile virus in the British Isles: an ecological review of candidate mosquito bridge vectors. Medical and veterinary entomology, 19(1), 2-21.

Novoseltsev, V. N., Michalski, A. I., Novoseltseva, J. A., Yashin, A. I., Carey, J. R., & Ellis, A. M. (2012). An age-structured extension to the vectorial capacity model. PloS one, 7(6), e39479.

Osório, H. C., ZÉ-ZÉ, L., Amaro, F., Nunes, A., & Alves, M. J. (2014). Sympatric occurrence of *Culex pipiens* (Diptera, Culicidae) biotypes pipiens, molestus and their hybrids in Portugal, Western Europe: feeding patterns and habitat determinants. Medical and veterinary entomology, 28(1), 103-109.

Ouyang, T. H., Yang, E. C., Jiang, J. A., & Lin, T. T. (2015). Mosquito vector monitoring system based on optical wingbeat classification. Computers and Electronics in Agriculture, 118, 47-55.

Parham, P. E., Waldock, J., Christophides, G. K., Hemming, D., Agusto, F., Evans, K. J., ... & Lenhart, S. (2015). Climate, environmental and socio-economic change: weighing up the balance in vector-borne disease transmission. Phil. Trans. R. Soc. B, 370(1665), 20130551

Rey, J. R., & Lounibos, P. (2015). Ecología de *Aedes aegypti* y *Aedes albopictus* en América y transmisión enfermedades. Biomédica, 35(2).

Roiz, D., Ruiz, S., Soriguer, R., & Figuerola, J. (2014). Climatic effects on mosquito abundance in Mediterranean wetlands. Parasites & vectors, 7(1), 333.

Rossati, A. (2017). Global warming and its health impact. The international journal of occupational and environmental medicine, 8(1 January), 963-7.

Rudolf, M., Czajka, C., Börstler, J., Melaun, C., Jöst, H., von Thien, H., ... & Tannich, E. (2013). First nationwide surveillance of *Culex pipiens* complex and *Culex torrentium* mosquitoes demonstrated the presence of *Culex pipiens* biotype pipiens/molestus hybrids in Germany. PloS one, 8(9), e71832.

Silva, D. F., Souza, V. M., Ellis, D. P., Keogh, E. J., & Batista, G. E. (2015). Exploring low cost laser sensors to identify flying insect species. Journal of Intelligent & Robotic Systems, 80(1), 313-330.

Thomas V. Gaffigan, Richard C. Wilkerson, James E. Pecor, Judith A. Stoffer & Thomas Anderson. (2018). Systematic Catalog of Culicidae. Walter Reed Biosystematics Unit. Retrieved from http://mosquitocatalog.org/

Valdés, V., Marquetti, M. D. C., Pérez, K., González, R., & Sánchez, L. (2009). Distribución espacial de los sitios de cría de *Aedes albopictus* (Diptera: Culicidae) en Boyeros, Ciudad de La Habana, Cuba. Revista Biomédica, 20(2), 72-80.

Villarreal, S. M., Winokur, O., & Harrington, L. (2017). The impact of temperature and body size on fundamental flight tone variation in the mosquito vector *Aedes aegypti* (Diptera: Culicidae): Implications for acoustic lures. Journal of medical entomology, 54(5), 1116-1121.

Villwock, S., & Pacas, M. (2008). Application of the Welch-method for the identification of two-and three-mass-systems. IEEE Transactions on Industrial Electronics, 55(1), 457-466.

Virginio, F., Vidal, P. O., & Suesdek, L. (2015). Wing sexual dimorphism of pathogen-vector culicids. Parasites & vectors, 8(1), 159.

Vogels, C. B. (2017). The role of *Culex pipiens* mosquitoes in transmission of West Nile virus in Europe (Doctoral dissertation, Wageningen University).

World Health Organitzation. (2014). A global brief on vector-borne diseases. Retrieved from http://www.who.int/campaigns/world-health-day/2014/global-brief/en/

Zheng, F., Zhang, G., & Song, Z. (2001). Comparison of different implementations of MFCC. Journal of Computer science and Technology, 16(6), 582-589.